ENERGY USAGE MODELING FOR HEATING AND COOLING OF OFF GRID SHELTERS

A Thesis
Presented to
The Academic Faculty

by

Daniel S. Lee

In Partial Fulfillment
of the Requirements for the Degree
Master of Science in the
George W. Woodruff School of Mechanical Engineering

Georgia Institute of Technology
December, 2017

ENERGY USAGE MODELING FOR HEATING AND COOLING OF OFF GRID SHELTERS

Approved by:

Dr. Yogendra Joshi, Advisor
School of Mechanical Engineering
Georgia Institute of Technology

Dr. Samuel Graham
School of Mechanical Engineering
Georgia Institute of Technology

Dr. Satish Kumar
School of Mechanical Engineering
Georgia Institute of Technology

Date Approved: September 27, 2017

ACKNOWLEDGEMENTS

First, I would like to thank my advisor, Dr. Yogendra Joshi, for his continuous guidance and support over the years working with him. I appreciate him for providing me with knowledge and wisdom for the successful completion of my degree. I would also like to thanks my two committee members, Dr. Samuel Graham and Dr. Satish Kumar, for their valuable support and advice. I thankfully acknowledge all the colleagues at National Renewable Energy Laboratory (NREL), Oak Ridge National Laboratory (ORNL), U.S Army Construction Engineering Research Laboratory (CERL), Off Grid Shelters LLC, and Outlast Technologies LLC for the assistance in providing valuable resources. I would also like to show appreciation to my co-workers, Kishore Karnik, Sumit De, Hampson Skinker, Wale Odukomaiya, Waylon Puckett, and Kam Yu Lee for their mutual participation in this project, and all my friends from METTL group who have provided helpful advices over my years of studies. Lastly, I would like to acknowledge the financial support from Department of Defense (DOD) and Office of Naval Research (ONR) throughout my degree.

TABLE OF CONTENTS

LIST OF TABLES

LIST OF FIGURES

SUMMARY

Most humanitarian missions, including disaster relief and refugee camps, as well as military missions, are off-grid and require the use of liquid fuels for local generation of electricity. For example, military forward operating bases (FOB) are typically located in remote areas, often in regions of conflict. Delivering fuel and other supplies to such FOBs can be both costly and risky. To lower the frequency of fuel delivery, it is important to predict the minimum amount of fuel needed for a given mission. Large portion of generated electricity in FOBs is consumed by heating, ventilation and air-conditioning (HVAC) demands of the temporary structures, known as shelters. Energy consumption of these shelters plays a crucial role in overall energy demand of the FOBs.

This research develops a method for modeling shelters that are deployed off the grid, and proposes a validation process to ensure that the energy performance of generated model corresponds to the actual shelter. The developed shelter models are then used to predict their energy usage in different geographical locations, before they are deployed. Shelter energy simulations are also integrated with advanced construction materials to seek energy performance improvements on existing shelter configurations.

CHAPTER 1. INTRODUCTION

1.1 Background

The Department of Defense (DOD) is the largest U.S government consumer of energy, spending billions of dollars per year on fuel. In FY2010, about 80% of the overall usage of fuel from the U.S government was by the DOD [1]. Along with the gradual increase of fuel costs, the amount of energy required for military operations has substantially increased. Increased demand for fuel generates challenges and risks to the military forces in operation. Transporting fuel to the forward operating bases (FOBs) is a time consuming and cost-intensive task, and with more time spent in transporting fuels, more soldiers are exposed to threats. Lowering the use of petroleum fuels would increase financial benefits for the DOD and would also decrease the risks to the soldiers, increasing combat effectiveness and mobility [1].

The two categories of energy usage of the FOBs are operational and installation energy. Operational energy is defined as the energy and associated systems, information, and processes required to train, move, and sustain forces and systems for military operations. According to the DOD, currently about 75% of overall energy use is operational energy, while 25% is installation energy. The usage of operational energy can be divided into three components: soldiers, vehicles/platforms, and basing [2, 3]. A large portion of the basing component of operational energy comes from heating, ventilation and air conditioning (HVAC) needs at forward operating bases. The largest non-propulsion consumers of liquid fuels are HVAC systems, which consume as much as 60 percent of the fuel allocated for a FOB during extreme weather periods.

Figure 1.1 Example of FOB Configuration (Fort Devens, MA) [3]
(Width of each shelter is approximately 20 ft.)

Need for energy to support HVAC systems in temporary structures is found not only at military bases, but also at non-military humanitarian camps in various emergency situations such as natural disasters. Most widely used emergency shelters are tents, having benefits of ease of transportation and installation. However, indoor living conditions are dependent on exposure to extreme weather depending on climate zones. Incorporation of HVAC systems to the shelters is commonly essential, in order to avoid further health-related problems to occupants [13]. Availability of reliable electrical power is not guaranteed in such emergency situations, and therefore effective management of fuel usage is crucial.

1.2 Past Efforts on Building Energy Modeling

1.2.1 Commercial Building Modeling

Much work has been done on energy analysis of commercial buildings, and there exists more than hundreds of building energy simulation tools. Modeling of commercial buildings was also done in the past, with the objective of energy savings. State-of-the-art building energy analysis includes introduction of new and unconventional materials or

systems into the model to seek energy performance advantages to the buildings. For example, solid-liquid phase change material (PCM) has been applied to building materials to enhance thermal performance. Alam et al. (2017) studied use of PCM in passive, active, and free cooling configurations, to compare its effectiveness in improving building thermal comfort. EnergyPlus and computational fluid dynamics (Ansys) simulations were performed [4]. Elarga et al. (2017) also introduced three different PCM materials integrated into roof space to investigate their performance by developing a numerical model and performing experiments [5].

Efforts have also been made to compare building energy simulation and experimental results. A study by Yousefi et al. (2017) showed that real life occupancy pattern has significant impact on the thermal energy usage inside residential building [6], suggesting the need for accurate occupancy assumptions in energy simulations. Parker et al. (2017) provided a methodology for using personal location metadata to generate accurate occupancy schedule that can be used as inputs to the simulation models [7]. Marshall et al. (2017) studied discrepancy between measured performance of building fabric and simulated model, and provided a method for modifying the model inputs to achieve better match in the results [8].

In addition, state-of-the-art computational algorithms have been introduced to building energy simulation and control to optimize energy consumption. Khanmirza et al. (2017) introduced model predictive control (MPC) as a temperature control method for the building, and also compared its efficiency with other intelligent methods [9]. Omar et al. (2017) presented self-learning algorithm for a residential building on a smart grid environment to estimate solar heat gain and temperature changes inside the building [10].

1.2.2 Shelter Energy Modeling

There have also been studies of building energy modeling for temporary shelters. Borge-Diez et al. (2013) performed computational fluid dynamics simulation to find cost reduction in concrete shelters using passive air-conditioning [11]. Kim et al. (2015) studied indoor thermal comfort level in hard-walled temporary housing unit, and compared it with regular container shelters. Field measured data for indoor air conditioning, and simulated results using EnergyPlus software for predicted energy demand were compared [12].

Few studies exist for soft-walled shelters, which are easily transported and rapidly deployed, allowing them to be used in both emergency disaster relief programs as well as military missions. Cordnaro et al. (2015) developed a simulation model of emergency shelters used by humanitarian organizations, which was calibrated with collected experimental data under un-conditioned climate. The study used an IDA Indoor Climate and Energy software to build the shelter model, and optimized solution for improved indoor air quality and suggested energy usage [13]. Crawford et al. (2012), developed a method of improving condition inside temporary shelters by creating shelter model using Environmental Systems Performance – research (EXP-r) software, and calibrating with test data [14].

Even though large portion of deployed military bases perform operations using soft -wall shelters as their main structures. Ghanmi (2014) examined energy usage and cost

management through an economic model [15]. However, whole building energy simulation was not performed during this study. A significant opportunity exists for energy optimization and operational energy consumption reduction at military bases through energy analysis using reliable military shelter energy models.

1.3 Research Objectives

The goal of this research is to develop a shelter energy usage modeling methodology, including the validation of the model. Parametric simulations are subsequently performed to study effectiveness of new materials in reducing heat loss, which will result in energy savings. In chapter 2, the core simulation tools used in the study, EnergyPlus and OpenStudio, are reviewed. Chapter 3 discusses the developed modular methodology for generating shelter energy models, including separate models for each components. In addition, validation of the shelter models is performed by comparing with results from field measurements. Parametric sensitivity analyses are performed for variables with higher uncertainties. In chapter 4, using the validated modeling framework, improved shelter configuration using three different new materials are investigated for energy savings. Also, the overall conclusions of this study are presented, as well as suggestions on future works.

CHAPTER 2. REVIEW OF THE SIMULATION SOFTWARE

As the simulation on this research is based on OpenStudio/EnergyPlus, this chapter provides review of the OpenStudio and EnergyPlus tool, and provides detailed explanation on their calculation.

2.1 EnergyPlus

EnergyPlus is a building energy simulation program targeted for design engineers or architects, to model and simulate the building energy performance. It was developed in collaboration with various DOE laboratories, academic and private institutions. The software was intended to succeed two previous energy simulation program, which are DOE-2 and Blast (Building Loads Analysis and System Thermodynamics). These two previous FORTRAN based tools were developed in the 1970s, and due to the high cost of maintenance, Department of Defense (DOD) decided to terminate their support of the software in the late 1990s. EnergyPlus was developed to meet the need for a newer energy system analysis tool written in a modern programming language, which is capable of simulating latest building designs and HVAC options, and also inherits the features of both DOE-2 and BLAST. Initially, EnergyPlus was written based on Fortran 90 standard. However, as of EnergyPlus version 8.2.0, the program has been fully translated into C++ language, which provides better development and maintenance [16].

EnergyPlus is capable of calculating energy consumption in buildings, which includes heating, ventilating, and air conditioning (HVAC) usage, as well as lighting and plug loads. It calculates the loads based on various input parameters such as building

formation, mechanical configuration, and environmental factors. Users can calculate full year simulation with sub-hourly time steps.

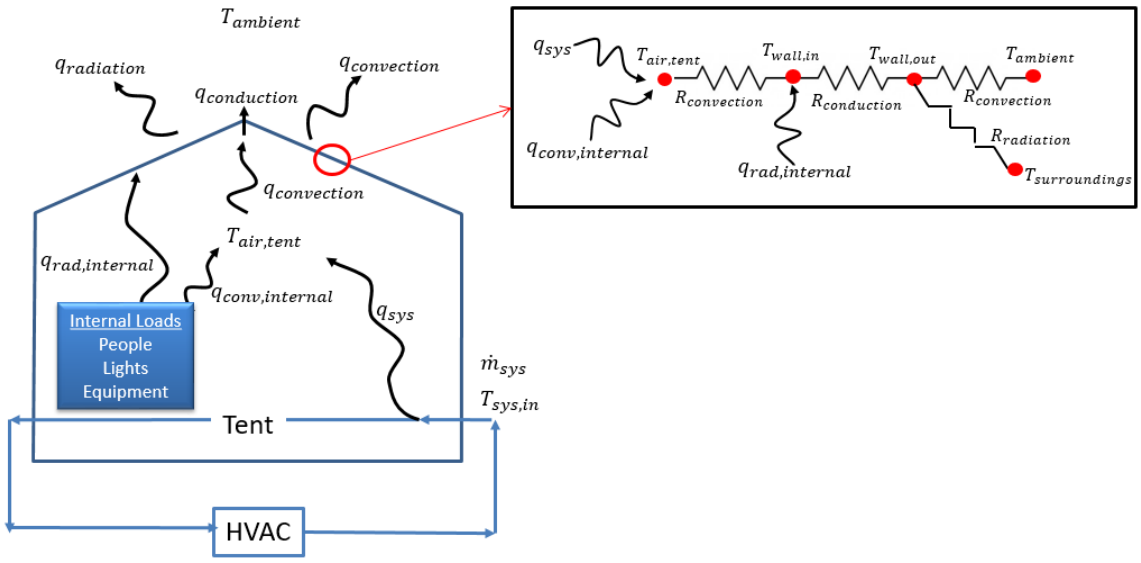

Figure 2.1 Heat Balance Based Solution of EnergyPlus

EnergyPlus uses heat balance-based solution, taking account of radiant and convective effect and calculating surface temperatures and condensation at each time step. It also provides solution based on transient heat conduction through building elements surfaces, three-dimensional ground heat transfer modeling, combined heat and mass transfer with moisture models, and thermal comfort models based on dry bulb temperature, humidity and activity. Furthermore, the software uses anisotropic sky model, daylighting controls, and advanced fenestration calculations as well as atmospheric pollution calculations, which result in improved accuracy in simulation of environmental effects [17].

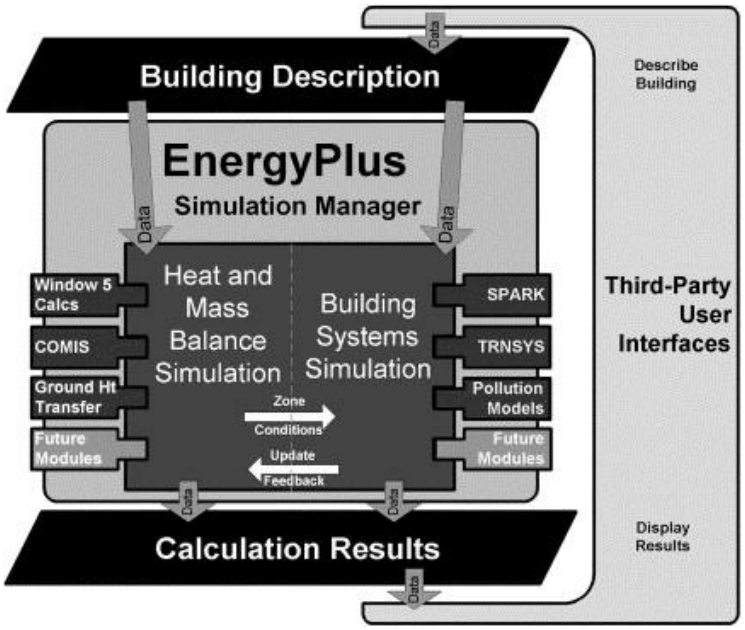

Figure 2.2 Modular Structure of EnergyPlus [10]

Another advantage of EnergyPlus is that it is an open source software with modular components. The source code of the program is intended to be accessed by developers in order to simultaneously improve the usability and accuracy of the program. The modularity provides users to develop a new models without requiring to modify other modules or the core software. It enables the developers to add new functions to the EnergyPlus tool.

2.2 OpenStudio

One shortcoming of the EnergyPlus is that it does not have a user interface. It is a simulation engine where input is given with simple ASCII texts. However, with its open source characteristic, it is possible for interface designers to produce a tool depending on

their needs [18]. OpenStudio is one of the graphical user interface (GUI) platforms that runs on EnergyPlus simulation engine. It is developed in collaboration by multiple national laboratories under U.S. Department of Energy, including National Renewable Energy Laboratory (NREL) and Oak Ridge National Laboratory (ORNL) to support combined energy simulation with EnergyPlus and Radiance (advanced daylight analysis engine). The software includes a set of components, which are OpenStudio application, OpenStudio SketchUp Plug-in, ResultsViewer and Parametric Analysis Tool. The OpenStudio SketchUp Plug-in works with Trimble's SketchUp software to enable fast and convenient method of drawing 3D building model geometries, which can be readily loaded into OpenStudio application [19].

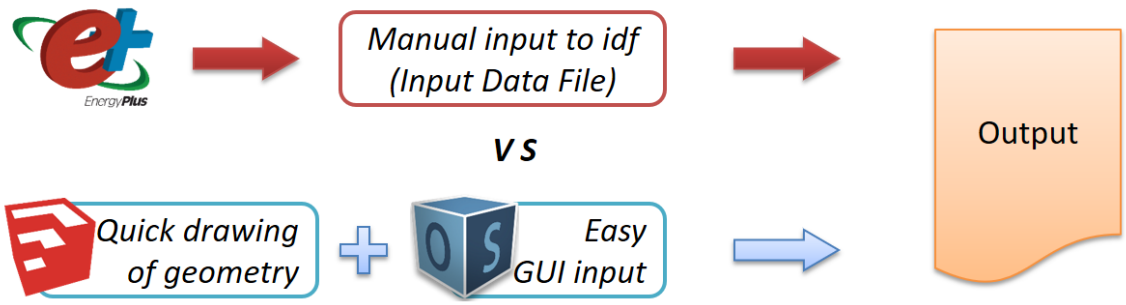

Figure 2.3 Benefit of Using OpenStudio

OpenStudio application then provides GUI to complete energy simulation inputs including construction, loads, schedules, as well as HVAC system loop. Once all inputs have been made and a completed OpenStudio model is generated, the model is translated into input

data files (idf) format, which is an input format of the EnergyPlus. The EnergyPlus engine then runs the simulation in the background, and after completion, OpenStudio retrieves output files which can be read using ResultsViewer. With ResultsViewer, a user can quickly browse and plot the simulation output. Parametric Analysis Tool allows automated parametric study on results using variable inputs.

The OpenStudio software is written in C++ language, and is an open source software allowing users to contribute in development and extension of the software. Furthermore, users can utilize custom scripts using Ruby language to create OpenStudio Measures that enable customization of OpenStudio models, and can be easily shared via embedded online library. Though OpenStudio is continuously being updated expanding its functionality, the GUI interface does not fully access the capability of the EnergyPlus. However, with use of OpenStudio Measures, a user can enable additional functions by writing custom commands using Ruby scripts.

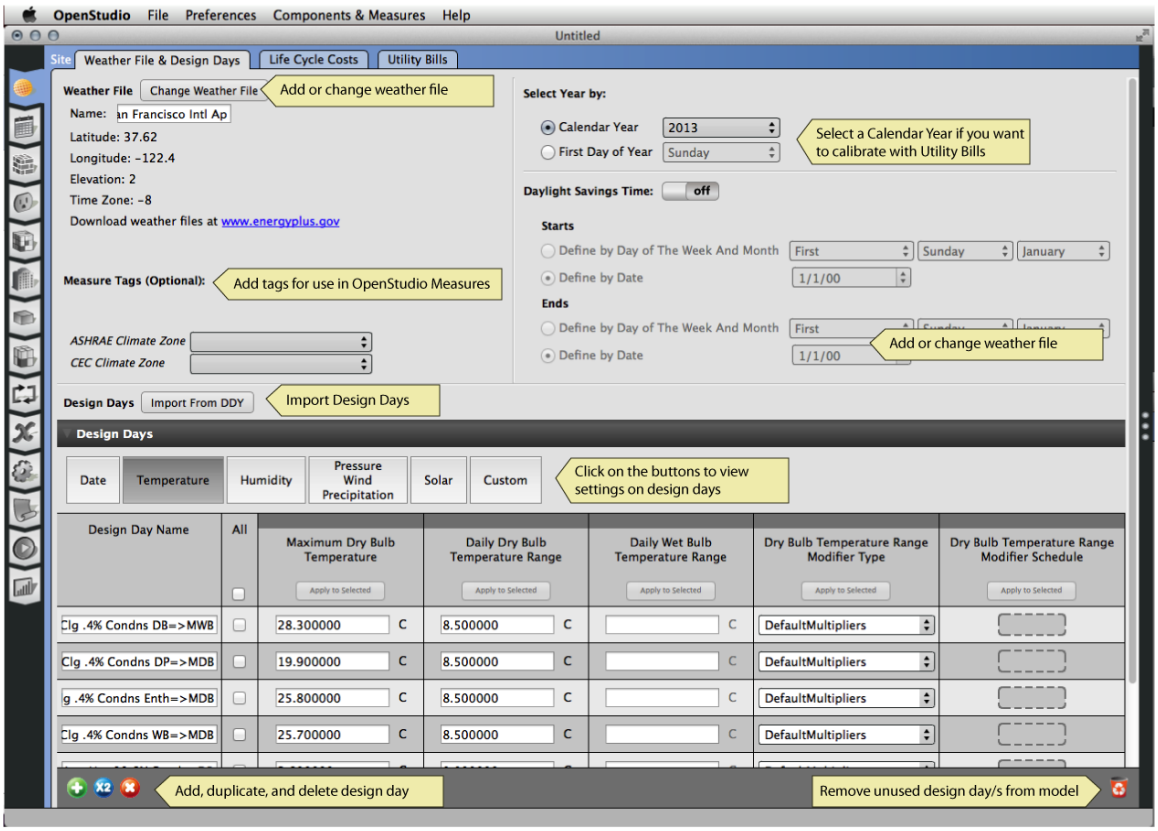

Figure 2.4 Example of OpenStudio Graphical User Interface

CHAPTER 3. SHELTER MODELING AND VALIDATION

Development of a thermal energy model for commercial and residential buildings can be easily done with readily available energy modeling software. However, only a few military shelters have been modeled by energy simulation tools, and the methods for generating these models vary greatly, which has resulted in inconsistent simulation results. This work aims to develop a best practice approach that will unify the procedure of shelter modeling.

Modeling expeditionary shelters, especially soft-walled tents, is challenging because the ambient environment must be taken into account. While conventional buildings depend more on conduction heat transfer, military shelters with their thinner surfaces, are significantly affected by convection and radiation heat transfer. Therefore, any model for military shelters must include precise convection and radiation properties. Also, with their direct thermal connection to the ground, the thermal interaction between ground temperatures and internal zone temperature of the shelter is significant. The research presented here will represent this interaction in a new model for the ground condition. It is also important to identify the infiltration value. Since these shelters usually have poor insulation and much higher infiltration rates compared to commercial buildings, classical methods of testing the infiltration rate cannot be easily applied to the shelters.

In this chapter, a detailed process of generating a shelter energy simulation model of a military shelter is developed, with consideration of important factors that can affect shelter energy performance including geometry, material properties, infiltration, HVAC system, and ground coupling. In addition, validation must be performed for the generated model in

order to ensure that the simulation result is reliable. This is done by acquiring field measured data, and comparing with the simulation for model with same conditions. These procedures are discussed in the following subsections.

3.1 Modeling Procedure

Each shelter model is a replication of a military structure (shelter) used in forward operating bases (FOB). The model has identical properties to an actual shelter, including geometry/dimensions, materials, construction, internal loads and infiltration. These models are generated in an OpenStudio model (OSM) format, which can be read by the OpenStudio software, a tool that is capable of generating energy usage profile of building structures.

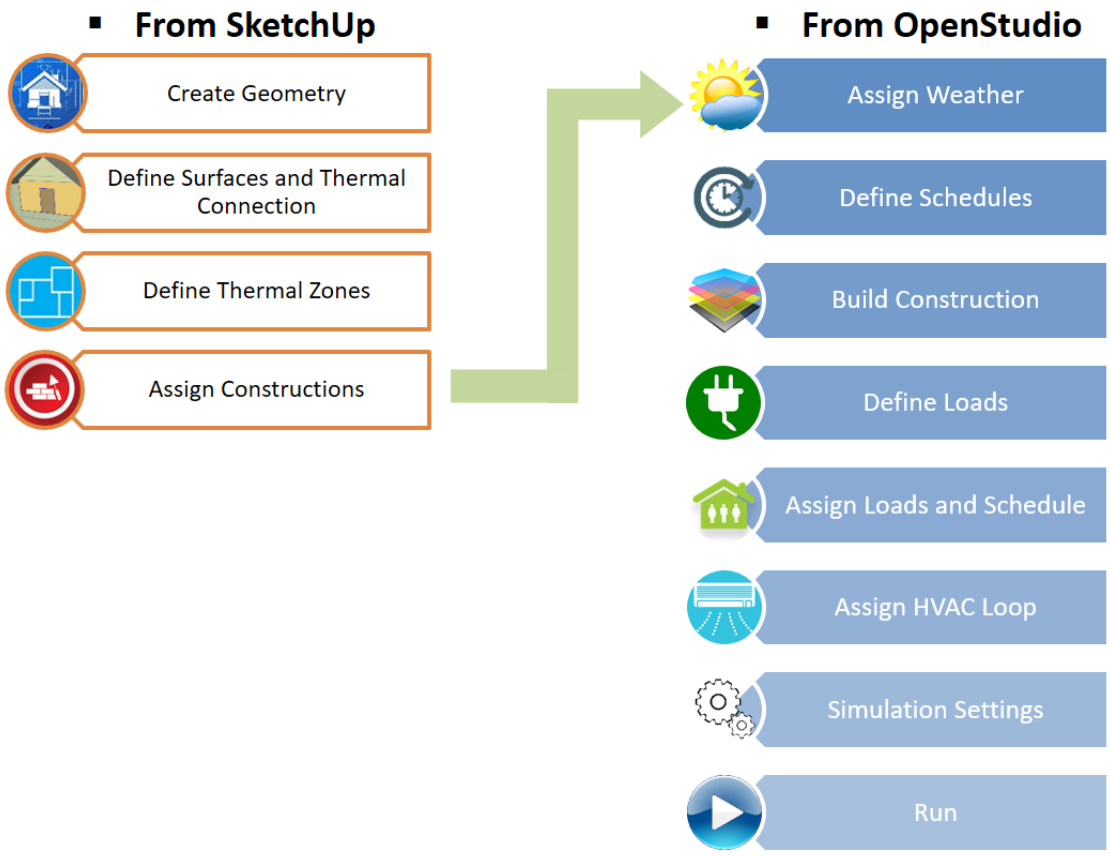

Figure 3.1 OpenStudio Model Generation Flow Chart

Figure 3.1 shows the flowchart of how a typical OpenStudio model is created. The modeling process follows the general procedure for generating an OpenStudio building model, but the following content is focused on unique inputs, that are different from modeling a conventional building structure.

3.1.1 Generating Shelter Envelope

The most important aspect of generating the shelter envelope is to acquire accurate dimension data for the shelter of interest. Manufacturers of military shelters may provide

the dimensions and floor plans of their product(s). If the shelter of interest is readily available, it is best to use measured dimensions for model input. In this study, Base-X model 305 shelter manufactured by HDT Global was selected as a test structure to perform outdoor measurements, and numerical simulations. Size data was acquired from the manufacturer datasheet [32].

The HDT Base-X 305 (X305) is a single-spaced soft-wall shelter, which consists of a layer of interior liner and an exterior cover. The shelter has interior floor area of 18’ in width and 25’ in length, and has a height of 10’ 6”. It is capable of accommodating 12 to 14 personnel, and can be utilized in various applications such as billeting, dining, and command structures. The diagram of the X305 shelter dimension is shown in Figure 3.2.

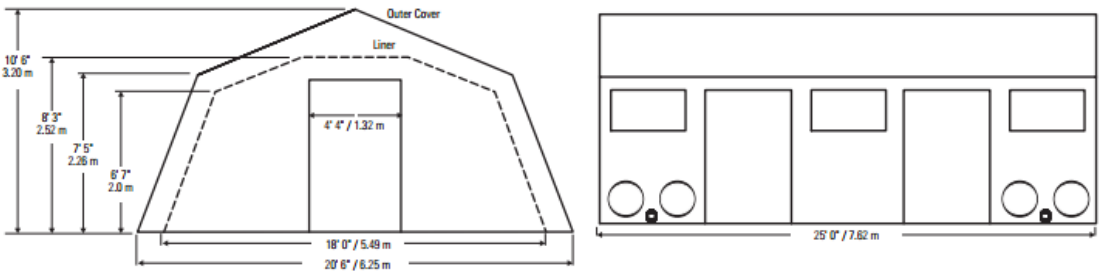

Figure 3.2 Blueprint of HDT Base-X 305 Shelter (HDT Global)

In order to generate an energy simulation model for OpenStudio, Trimble SketchUp software is used to generate the envelope of the shelter, which can be imported into OpenStudio for further configurations. SketchUp is an intuitive 3D drawing tool, and by

utilizing OpenStudio plug-in for SketchUp, the software can generate OpenStudio building objects and can also insert several other important OpenStudio input objects.

The shelter envelope is created by following the regular procedure for drawing 3D building model using SketchUp tool. However, there are few different key points which need to be followed in order to use the 3D model in OpenStudio. First, OpenStudio plug-in for SketchUp has to be installed. This is done automatically by firstly installing SketchUp software, and then installing the OpenStudio software. Once the plug-in is ready, an OpenStudio space can be generated from OpenStudio toolbar. All of the components that are drawn inside this space will be recognized as OpenStudio objects.

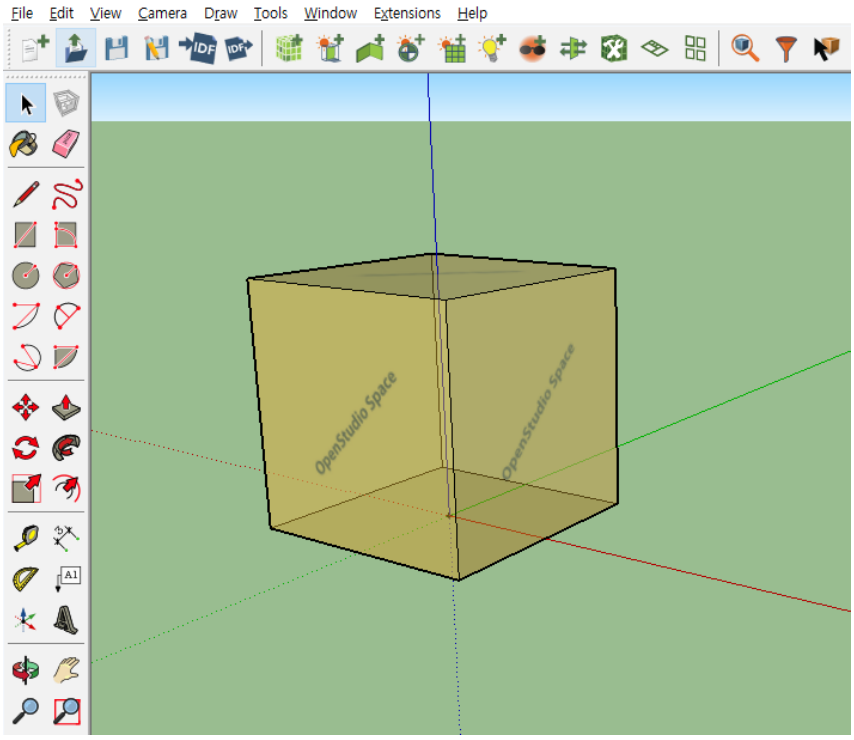

Figure 3.3 Example of SketchUp Interface – Generating OpenStudio Space

Once the HDT Base-X305 model geometry is created, thermal zones have to be assigned. The thermal zone is sections of interior space that is usually divided physically by walls, or for a shelter, by liners. In X305 model, there are two thermal zones. 'Main zone' is an actual living space, occupied by personnel and most of interior equipment and lighting. The HVAC will be attached to this zone to condition the air inside the space. Therefore the main zone is also called 'conditioned zone'. The 'Gap zone' is a narrow space between outer cover and inner liner. The temperature of this space is not controlled, thus it is also called 'unconditioned zone'. During OpenStudio simulation, a thermal zone is assumed to be in a well-mixed state, having uniform temperature throughout the single thermal zone space.

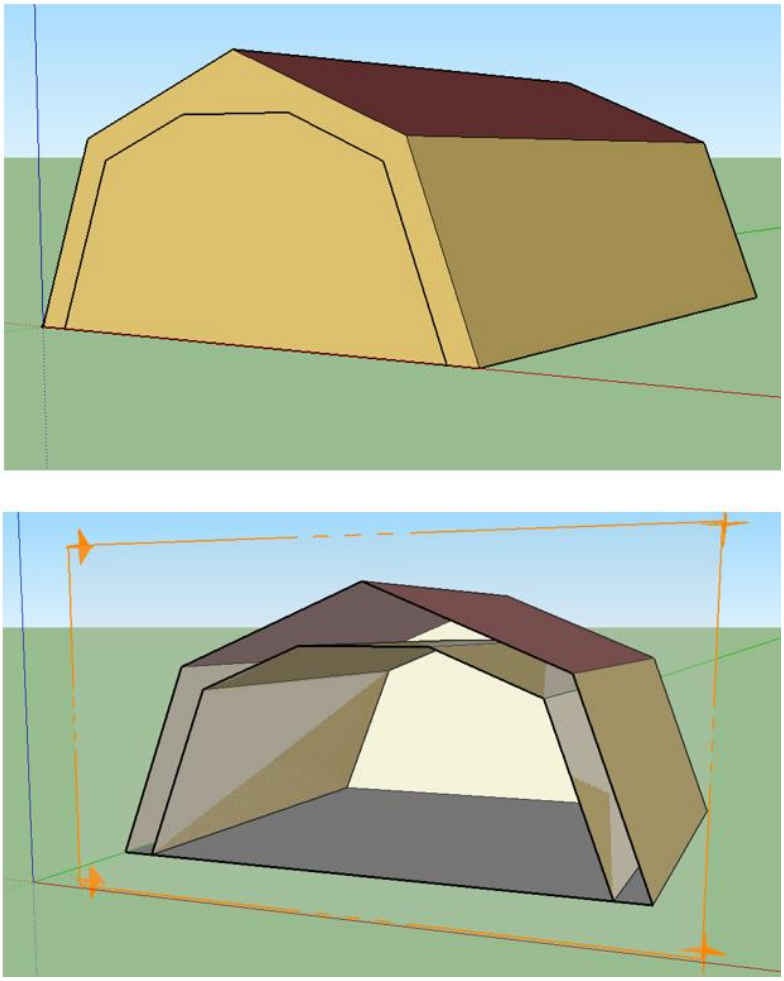

Figure 3.4 HDT Base-X 305 Model Generated in SketchUp and the Cross-sectional View

With the appropriate thermal zones placed, the envelope of the shelter is generated and is prepared for other inputs.

3.1.2 Measuring Material Properties

In order to have accurate simulation results, it is important to input precise material properties to the model construction. Material properties can be acquired by referencing general property tables, or can be measured directly from actual shelter material. In this

study, laboratory measurements were conducted to measure the shelter liner thermal conductivity using material samples received from Off Grid Shelters of the deployed X305 shelter and of a smaller soft-walled tent. In addition to the shelter materials, an aerogel insulation material and a radiant barrier sample were also received (Figure 3.5), and their properties were measured to investigate potential improvement in energy efficiency using these advanced materials.

Figure 3.5 Received Sample Materials for Thermal Conductivity Measurement

The experimental set-up consists of a film heater, which provides heat through to the sample material, and the thermoelectric module (Peltier device), which acts as the heat sink. The film heater is sandwiched between two identical pieces of the sample material, ensuring all of the heat generated is dissipated through the sample material. The

thermoelectric module in turn covers the outer surface of sample and the heater layer, creating a symmetric configuration. Pad type graphite thermal interface material (TIM) of 0.127mm (0.0050 inch) thickness is inserted at each interface to reduce the thermal contact resistance. Figure 3.6 shows the layout of the measurement setup, and the location of thermocouples. T type Thermocouples with 0.254mm (0.010 inch) diameter were used.

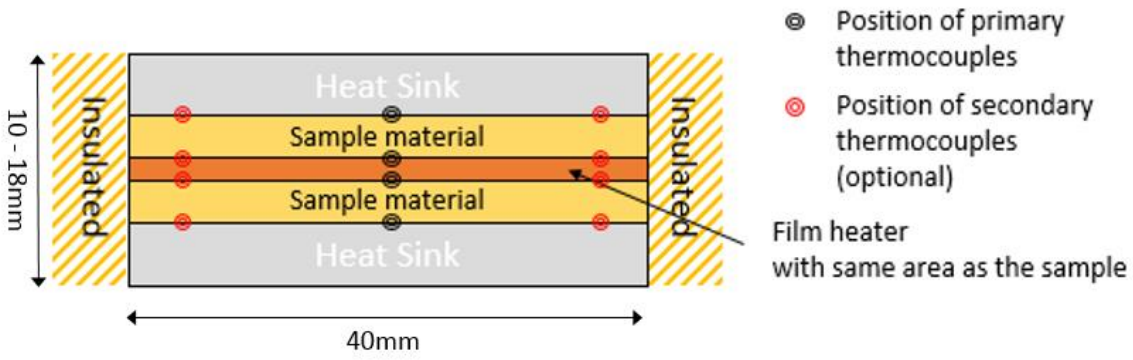

Figure 3.6 Schematic of Thermal Conductivity Measurement Setup

In this study, the heater power of approximately 19W was maintained throughout the measurement. The thermoelectric heat sink is maintained at a temperature of 23^{o}C in these tests. After steady state is achieved, as defined by temperature change of less than 0.5^{o}C on each measurement points during 15 minute period, the temperature at each side of the sample is measured. By measuring the temperature difference between the two sides and the total heat input, it is possible to calculate the effective thermal conductivity and the thermal resistance of the sample material using Equations (1) through (3), which are based on an assumption of 1-D heat transfer. Additional thermocouple nodes are placed at the edges of the sample interfaces in order to ensure that the heat from the film heater is

distributed evenly throughout the heater surface, which is a critical factor in 1-D heat transfer assumption.

$$Q = \frac{kA\Delta T}{t} \tag{1}$$

$$k = Q\frac{t}{A\Delta T} \tag{2}$$

$$R = \frac{\Delta T}{Q} = \frac{t}{k} \tag{3}$$

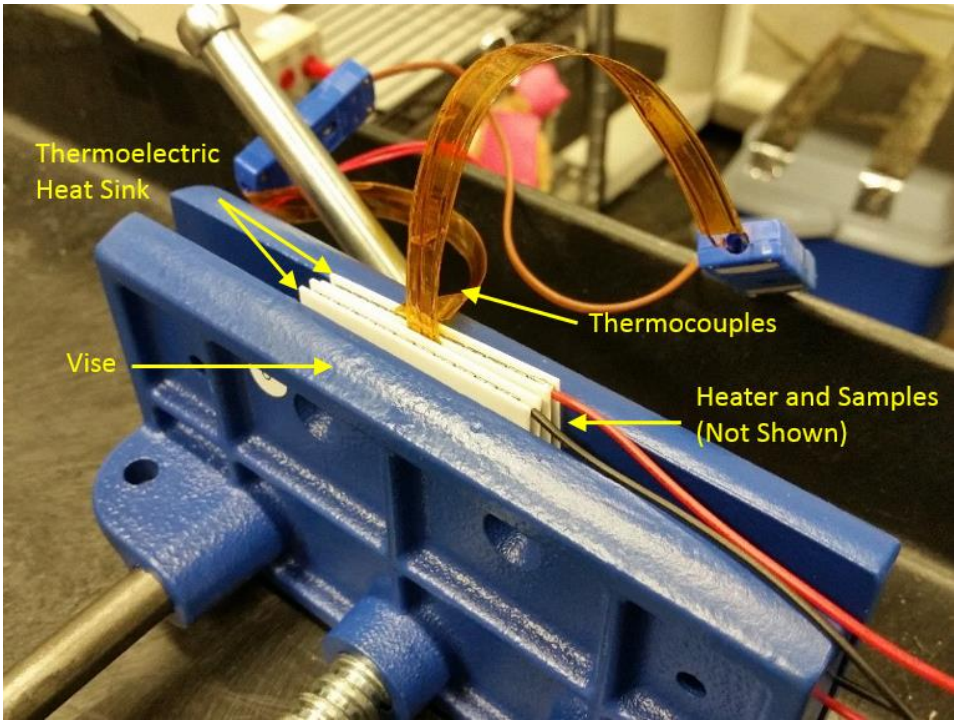

Figure 3.7 Measurement Configuration

All layers of the test sample are held together, using a parallel vise, giving minimal normal pressure to the surface. Interface pressure is measured using a force sensitive resistor (FSR 400 5mm circle, Interlink Electronics), and maintained at 38 kPa. Fiberglass insulation is then inserted around the edges to reduce heat loss. Figure 3.7 is a photo of measurement setup, but without the fiberglass insulation materials to show the various layers.

Since the sample materials are mostly soft liners such as fabrics or synthetic fibers, it was found that the measurement of effective thermal conductivity highly depends on the normal pressure applied on the measurement layers. Especially, aerogel insulation and radiant barrier showed large differences, due to their porous characteristics. A pair of force sensitive resistors was attached in between the outer surface of the heat sink and the clamp,

to measure and to control the normal pressure applied to the test layers for uniformity throughout each measurement.

Results of the effective thermal conductivity measurements are shown in Table 3.1. Thickness measurements have relative error of ±0.56%, temperature and heat flux measurements have relative error of ±7.8% and ±0.59% respectively. Resulting effective thermal conductivity and thermal resistance values have uncertainty of ±8.8% and ±8.4%, respectively [34-36].

Table 3.1 Measurement Results – Effective Thermal Conductivity and Thermal Resistance

Material	Thickness (mm)	ΔT (K)	Heat Flux (W)	k (W/mK)	R (m^2K/W)
BaseX Liner	0.229	1.5	0.95	0.091	0.0025
BaseX Shell	0.330	3.2	0.97	0.064	0.0052
BaseX Floor	0.381	3.7	0.96	0.063	0.0061
Prototype Liner	0.330	2.2	0.90	0.085	0.0039
Prototype Shell	0.368	2.7	0.98	0.082	0.0045
Prototype Floor	0.394	2.5	0.95	0.095	0.0041
Aerogel insulation	1.270	8.2	0.91	0.088	0.014
Radiant Barrier	4.191	27.5	0.71	0.068	0.062

Measured properties are then inserted to the shelter model using the OpenStudio user interface (Figure 3.8). Since these liner materials are thin and light weight, they are inserted as 'No mass materials'. Input for no mass materials requires thermal resistance value, which can be calculated using measured thermal conductivity and thickness of the material. The thermal, solar and visible absorptance data was acquired form a report from Construction Engineering Research Laboratory (CERL) of US Army Corps of Engineers

and NREL, which conducted property measurement of HDT AirBeam 2032 shelter using similar liner materials [20].

Table 3.2 Roughness and Absorptance Properties of the Materials [20]

Property	Units	Exterior Shell		Inner Liner	
		Outer Surface	Inner Surface	Outer Surface	Inner Surface
Roughness	-	Medium Smooth	Medium Smooth	Medium Smooth	Medium Smooth
Thermal absorptance	Fraction	0.897	0.90	0.889	0.899
Solar absorptance	Fraction	0.571	0.9	0.13	0.13
Visible absorptance		0.6	0.9	0.13	0.13

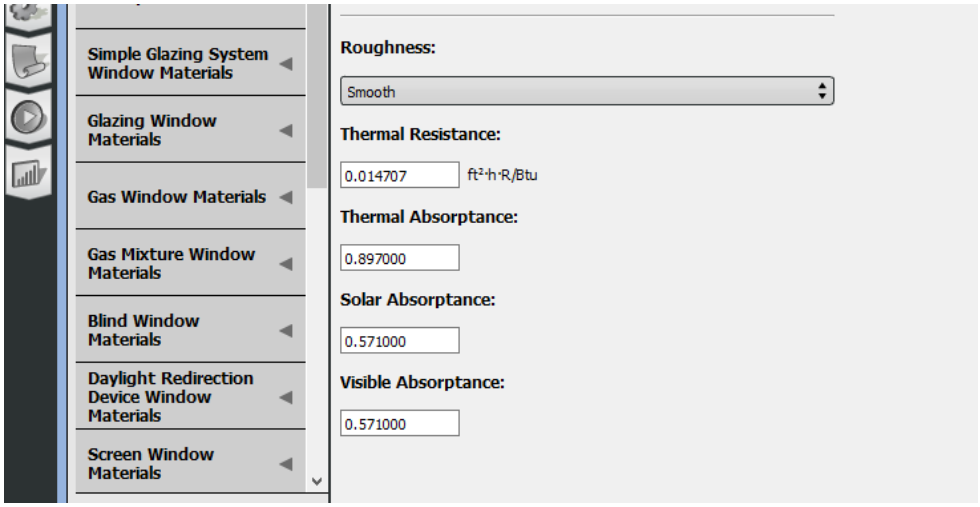

Figure 3.8 Material Properties Input in OpenStudio Application

The materials are then put in layers to form a cross-sectional construction (Figure 3.9). Each construction is assigned to surfaces of the shelter model.

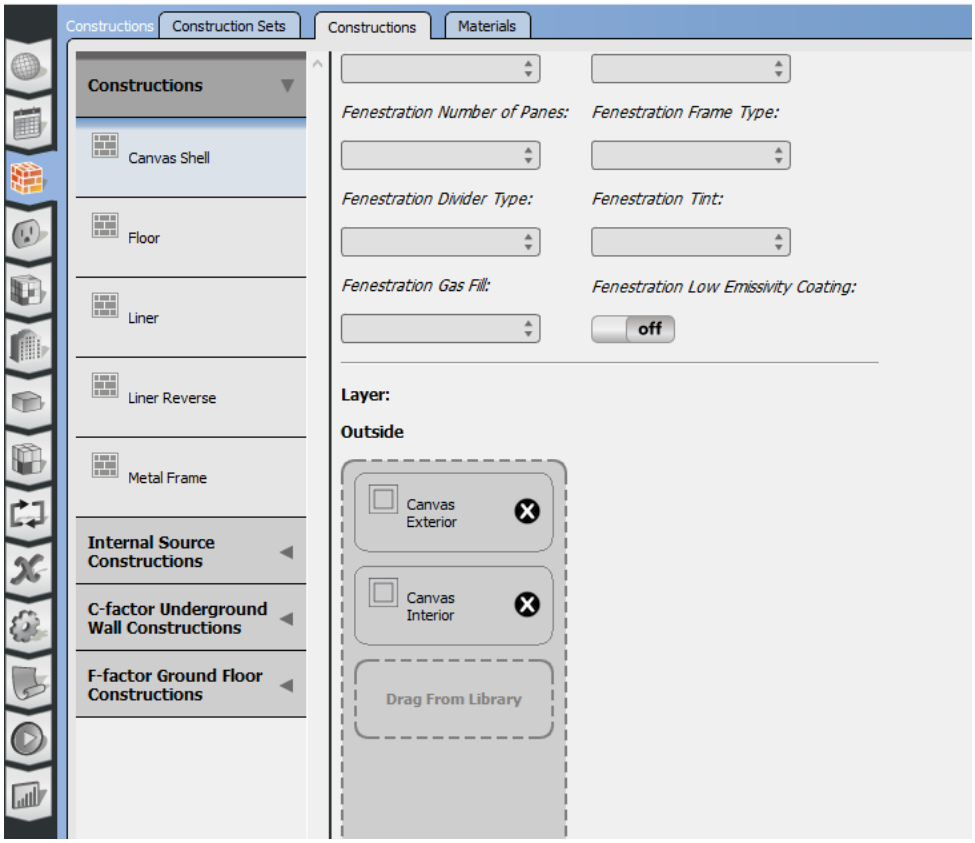

Figure 3.9 Assigning Construction Layers

3.1.3 Location and Weather

Environmental factors are important in energy simulation since difference in location will result in different weather, atmospheric pressure, and solar radiation inputs. Following the field measurements performed by Off Grid Shelters LLC, the location was set to New Hampshire.

For the weather inputs, OpenStudio shares same weather input format with EnergyPlus. The EnergyPlus requires specific format of weather data input file, which is called EnergyPlus Weather file (EPW). The EPW files contains hourly information of meteorological data and solar radiation data sets for a whole year. The file can be generated from locally measured data, modified to follow the format. However if the data is not available, EnergyPlus website (energyplus.net) provides typical meteorological weather files based on historical measurement at different locations (more than 2,000) around the globe, and a user can download and use one of the provided EPW files for the closest location. An example of weather file format is shown in Figure 3.10. The first eight lines include general information on the weather file such as location, monthly ground temperatures and design conditions. Following lines contain arrays of hourly weather information, each line representing every hour.

As discussed in section 3.2, even though field measurement has provided local weather data at the temporary weather station, the data was not enough to fully create an EPW formatted file, lacking some information such as ground temperatures. Therefore, in this study an EPW file from the website was used as a default, with closest available location being Concord Municipal Airport, NH. Wherever available, the default data point was replaced with the measured data. Using this process, a full year EPW file can be created, despite the fact that the measurement was only available for less than 20 days period. However, the simulation is run only for that specific time window.

```
LOCATION,Concord Municipal Arpt,NH,USA,TMY3,726050,43.2,-71.5,-5,106,,,,,,,,,,,,,,,,,,,,,,,,,,,,,,
DESIGN CONDITIONS,1,Climate Design Data 2013 ASHRAE Handbook,,Heating,1,-19.8,-16.9,-26.1,0.4,-17.
TYPICAL/EXTREME PERIODS,6,Summer - Week Nearest Max Temperature For Period,Extreme,7/15,7/21,Summe
GROUND TEMPERATURES,3,0.5,,,,-3.46,-4.58,-2.6,0.5,8.61,14.86,19.08,20.37,18.18,13.32,6.83,0.81,2,,
HOLIDAYS/DAYLIGHT SAVINGS,No,0,0,0,,,,,,,,,,,,,,,,,,,,,,,,,,,,,,,,,,,,,,,,,,,,,,,,,,,,,,,,,,,,,,,,,,
COMMENTS 1,Custom/User Format -- WMO#726050; NREL TMY Data Set (2008); Period of Record 1973-2005
COMMENTS 2,-- Ground temps produced with a standard soil diffusivity of 2.3225760E-03 {m**2/day},,
DATA PERIODS,1,1,Data,Sunday,1/ 1,12/31
1991,1,1,1,60,?9?9?9?9E0?9?9?9?9?9?9?9?9?9?9?9?9?9?9?9*9*9,-11.1,-15.6,66,102100,0,0,198,0,0,0,0,0
1991,1,1,2,60,?9?9?9?9E0?9?9?9?9?9?9?9?9?9?9?9?9?9?9?9*9*9,-11.7,-15.6,70,102100,0,0,197,0,0,0,0,0
1991,1,1,3,60,?9?9?9?9E0?9?9?9?9?9?9?9?9?9?9?9?9?9?9?9*9*9,-12.2,-16.1,70,102200,0,0,195,0,0,0,0,0
1991,1,1,4,60,?9?9?9?9E0?9?9?9?9?9?9?9?9?9?9?9?9?9?9?9*9*9,-12.8,-15.6,77,102200,0,0,193,0,0,0,0,0
1991,1,1,5,60,?9?9?9?9E0?9?9?9?9?9?9?9?9?9?9?9?9?9?9?9*9*9,-14.4,-15.6,90,102200,0,0,189,0,0,0,0,0
1991,1,1,6,60,?9?9?9?9E0?9?9?9?9?9?9?9?9?9?9?9?9?9?9?9*9*9,-14.4,-16.1,85,102300,0,0,188,0,0,0,0,0
1991,1,1,7,60,?9?9?9?9E0?9?9?9?9?9?9?9?9?9?9?9?9?9?9?9*9*9,-15.0,-16.7,85,102400,0,0,186,0,0,0,0,0
1991,1,1,8,60,?9?9?9?9E0?9?9?9?9?9?9?9?9?9?9?9?9?9?9?9*9*9,-15.0,-16.1,90,102400,45,955,193,11,47,
1991,1,1,9,60,?9?9?9?9E0?9?9?9?9?9?9?9?9?9?9?9?9?9?9?9*9*9,-10.0,-13.3,74,102500,234,1415,212,98,2
1991,1,1,10,60,?9?9?9?9E0?9?9?9?9?9?9?9?9?9?9?9?9?9?9?9*9*9,-8.3,-13.3,64,102500,399,1415,216,228,
1991,1,1,11,60,?9?9?9?9E0?9?9?9?9?9?9?9?9?9?9?9?9?9?9?9*9*9,-5.6,-12.8,53,102400,513,1415,218,325,
1991,1,1,12,60,?9?9?9?9E0?9?9?9?9?9?9?9?9?9?9?9?9?9?9?9*9*9,-3.9,-13.3,44,102300,566,1415,223,371,
1991,1,1,13,60,?9?9?9?9E0?9?9?9?9?9?9?9?9?9?9?9?9?9?9?9*9*9,-2.8,-13.3,40,102200,554,1415,227,361,
1991,1,1,14,60,?9?9?9?9E0?9?9?9?9?9?9?9?9?9?9?9?9?9?9?9*9*9,-2.2,-12.2,42,102200,480,1415,246,173,
1991,1,1,15,60,?9?9?9?9E0?9?9?9?9?9?9?9?9?9?9?9?9?9?9?9*9*9,-2.2,-12.2,42,102100,347,1415,265,69,0
1991,1,1,16,60,?9?9?9?9E0?9?9?9?9?9?9?9?9?9?9?9?9?9?9?9*9*9,-2.2,-11.7,44,102100,167,1415,266,32,0
1991,1,1,17,60,?9?9?9?9E0?9?9?9?9?9?9?9?9?9?9?9?9?9?9?9*9*9,-2.8,-11.1,49,102100,10,460,264,1,0,1,
1991,1,1,18,60,?9?9?9?9E0?9?9?9?9?9?9?9?9?9?9?9?9?9?9?9*9*9,-2.8,-11.7,46,102100,0,0,263,0,0,0,0,0
1991,1,1,19,60,?9?9?9?9E0?9?9?9?9?9?9?9?9?9?9?9?9?9?9?9*9*9,-3.3,-11.7,48,102100,0,0,261,0,0,0,0,0
1991,1,1,20,60,?9?9?9?9E0?9?9?9?9?9?9?9?9?9?9?9?9?9?9?9*9*9,-3.3,-11.1,51,102000,0,0,262,0,0,0,0,0
```

Figure 3.10 Example of EPW Weather File

3.1.4 Loads and Infiltration

Loads are internal gains that influence the HVAC energy consumption. This includes people, lightings and other internal zone equipment. In the field test of the Base-X305, the shelter was not occupied most of the time and had no lighting equipment inside. Therefore, only the internal electric equipment object was created to model the measuring equipment and air conditioning unit.

Infiltration can also have similar effect on loads, since the loss in indoor air will change the comfort level resulting in higher HVAC demand. Air leakage can cause up to 50 percent of the heat loss in building structures, increasing energy consumption by the HVAC equipment [21]. Since soft-walled shelters are poor in air-tightness, they have

significant air leakage, which impacts the indoor comfort, and heating and cooling demands. Since air infiltration plays a more significant role in soft-shell shelters compared to conventional hard-walled buildings, it is essential that it is quantified and its effect reflected in the simulation model. In order to measure the air infiltration, two methods are generally used, the tracer gas method, and the fan pressurization method. The former is more accurate, but costly and requires trained experts [22]. The fan pressurization method is easier to perform with less cost, and therefore it is commonly employed for expeditionary shelters.

One of the most common fan pressurization methods is the blower door test. The leakage of structure envelope is measured by pressurizing and depressurizing the structure with fan attached to a door. During the test, the envelope is gradually pressurized/depressurized up to 50 Pa and the volume flow rate of the fan is measured in cubic feet per minute (CFM). Using the known shelter volume, an air change per hour (ACH) value at 50 Pa can be obtained. The CFM or ACH value can be converted to other convenient infiltration units. Since the shelters are usually built with thin flexible materials and metal frames, using high pressure difference of 50Pa may cause collapse or damage, especially during the depressurization. Therefore, in the data utilized in this study from Iacocca [30], a lower pressure was used to measure consecutive data points, and the values were extrapolated to derive equivalent airflow rate at 50Pa. As a result of the measurement, an average of 49.24 ACH at 50Pa was acquired [30]. Figure 3.11 shows the picture of blower door test equipment installed at a door flap section of the X305 shelter. A fan is installed at the hole shown on right bottom side of the door to pressurize or depressurize the shelter.

Figure 3.11 Base-X 305 Shelter with Blower Door Test Equipment Installed [30]
(Door height is approximately 7 ft.)

The test results are shown in Table 3.3.

Table 3.3 Blower Door Test Results [30]

Base-X 305 Shelter Pressure Testing Results 2015-09-04		
Temperature	~80F	
Baseline pressure	-0.6 Pa	
Shelter volume (cu. ft.)	2,790	
Results	Pressure	CFM @ 50 Pa
Negative	-33.1	3410
Positive	59.2	1169
Air Changes/hour @ 50 Pa		
Negative	73.33	
Positive	25.14	
Average	49.24	

Among the inputs for air infiltration that OpenStudio provides, the effective leakage area (ELA) model is a convenient and more accurate method for calculating the infiltration value in units of cm^2. With the ELA object, OpenStudio is able to calculate the actual

infiltration value using indoor/outdoor temperature difference and wind speed at a given time step, based on correlation derived by work of Sherman and Grimsrud (1980) [23, 24].

$$Infiltration = \frac{A_L}{1000}\sqrt{C_s\Delta T + C_w(WindSpeed)^2} \quad (4)$$

Equation (4) shows the correlation where A_L is the effective leakage area in cm^2, ΔT is the average difference between indoor and outdoor air temperature in Celsius. C_s is a stack coefficient, which is 0.000145[$(L/s)^2/(cm^4 \cdot K)$] for one story building, and C_w is wind coefficient, which is 0.000319[$(L/s)^2/(cm^4 \cdot (m/s)^2)$] for shelter class 1 (no obstruction or local shielding), single story building [25].

Concept of effective leakage area is that the overall leakage of the building will be equivalent to air leak through single opening of an orifice hole in the structure envelope with certain cross-sectional area. The ELA model requires input of effective air leakage area in cm^2 at 4Pa. Since the measured value of blower door test is given in air flow rate at 50Pa, it is necessary to convert the air flow rate to effective leakage area at 50Pa by following Equation (5) [25]

$$A_{L-50Pa} = B\frac{CFM_{50}}{C_D}\sqrt{\frac{\rho}{2\Delta p_{r-50Pa}}} \quad [cm^2] \quad (5)$$

where B is a unit conversion factor (0.186), CFM_{50} is the measured air flow rate at 50Pa, and C_D is discharge coefficient (1.0). ρ [kg/m^3] is the density of air at the measured location (Strafford, NH), and $\Delta p_{r\text{-}50Pa}$ is the reference pressure in inches of water at 50Pa (0.201). The ELA at 50Pa calculates 1176.454 cm^2.

$$A_{L-4Pa} = A_{L-5Pa}\left(\frac{\Delta p_{r-4Pa}}{\Delta p_{r-50Pa}}\right)^{n-0.5} \quad (6)$$

Consecutively, using Equation (6) [25], the ELA at 50Pa can be converted to ELA at 4Pa where $\Delta p_{r\text{-}4Pa}$ is the reference pressure in inches of water at 4Pa (0.016), and *n* is the pressure exponent (0.65). The calculation gives ELA at 4Pa to be 805.45 cm^2, which can now be used as input for OpenStudio infiltration object.

3.1.5 ECU System Modelling

The Environmental Control Unit (ECU) maintains desirable temperature range within the shelter envelope. In order to simulate and validate the shelter performance with field-measured data, it is necessary to incorporate a model of the ECU system into the simulation model. OpenStudio provides various templates to be used as a starting point, however additional inputs are needed to tune the ECU model. This includes specification of the equipment such as cooling/heating capacity, rated coefficient of performance (COP), rated sensible heat ratio, fan efficiency, and flow rate. In addition, it requires inputs of cooling performance curves, which are sets of quadratic or biquadratic curve that represent important cooling coil characteristic including cooling capacity and energy input ratio data. In other words, a performance curve enables OpenStudio to generate a plot in 3D space where a desired output value such as cooling capacity can be given for each combination of inputs of outdoor dry bulb temperature and return air wet bulb temperature. This allows the software to determine the instant characteristic of ECU system at each time step, with current wet bulb and dry bulb temperatures. OpenStudio allows users to input coefficients of each curve and allows the simulation to calculate the output based on generated curves.

Most of the ECU manufacturers provide general specification of their products, and it is relatively easier to obtain inputs such as cooling capacity and COP values. However, not many products are provided with detailed performance characteristics and performance curves because the curves have to be fitted from the data points gathered after conducting extensive physical experiments on various combinations of environment conditions. Given such data points, it is possible to derive performance curve coefficients using regression analysis of the data.

In this study, the field measurement was done in cooling period (hot weather period) with an air conditioning unit and without heating capability [30]. The system used is Office Pro 60 manufactured by MovinCool (Figure 3.12). The technical specification is given as in Figure 3.13, and also performance plot is provided for cooling capacity and power consumption curve (Figure 3.14). The rating condition is given as 35°C and 60% RH. With these pieces of information, data points were sampled and put into regression analysis spread sheet (Figure 3.15). Using the built in data analysis function of Microsoft Excel, The biquadratic coefficient for the cooling performance curve and energy input ratio curve is derived (Figure 3.16).

Figure 3.12 MovinCool Office PRO 60 Portable Cooler [31]

4. SPECIFICATIONS

4.1 Technical Specifications

ITEM			SPECIFICATIONS
Electronic Features	Control Panel		Electronic
	Thermostat Control		Electronic
Cooling Capacity*1	Capacity-208/230 V		58500/60000 Btu/h (17145/17585 W)
Refrigerant Circuit	Compressor	Compression Type	Hermetic Scroll
		Motor Rated Output at 230 V	3.89 kW
	Evaporator		Plate Fin
	Condenser		Plate Fin
	Refrigerant Control		Capillary Tube
Refrigerant/Enclosed quantity			R-410 A/3.97 lb (1.80 kg)
Ventilation Equipment For Evaporator	Fan Type		Centrifugal
	Max. Air Flow-high/low		1940/1770 CFM (3300/3000 m^3/h)
	Motor Rated Output-high/low at 230 V		0.60/0.33 kW
	Max. External Static Pressure		0.9 IWG (224 Pa)

Figure 3.13 Sample of Specification Provided by Manufacturer [31]

4.2 Characteristics (at 230 V)

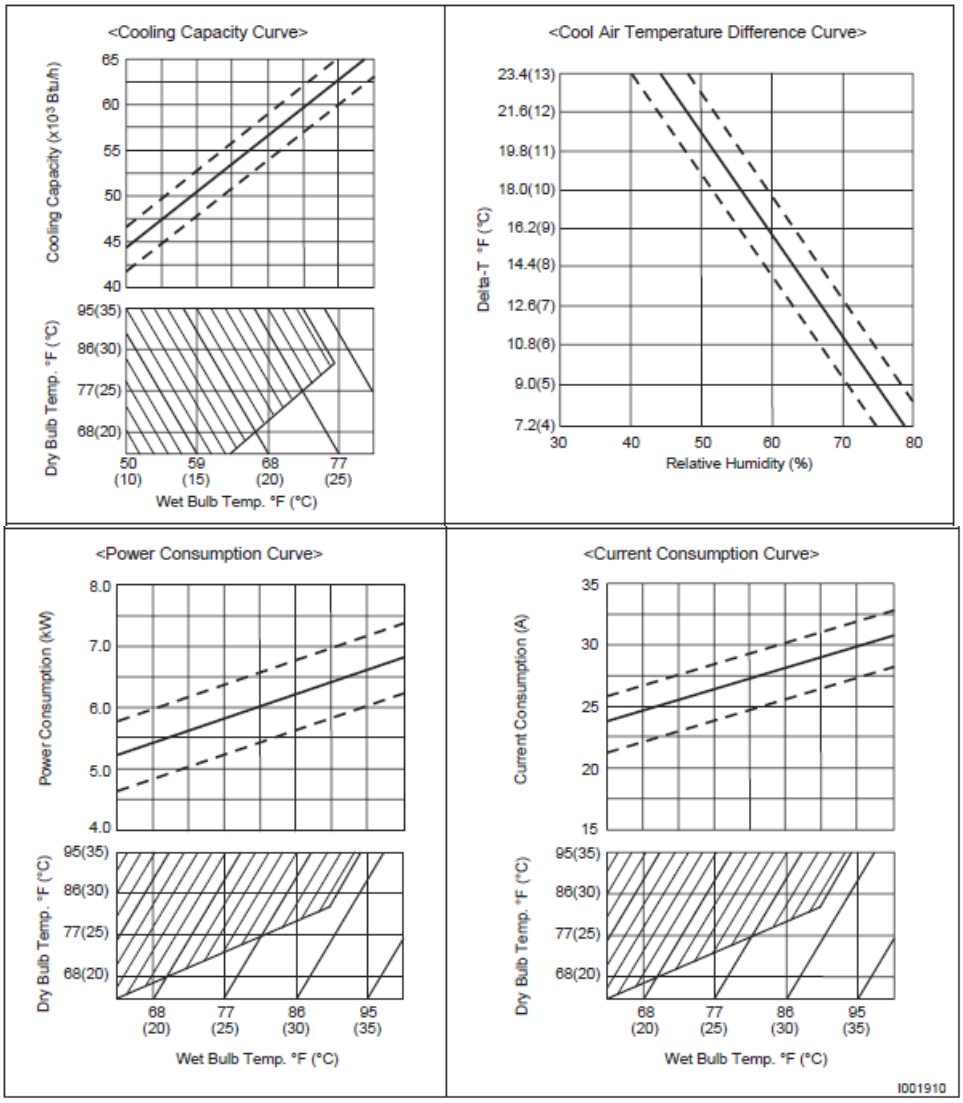

Figure 3.14 Characteristic Performance Curve of the AC Unit [31]

Return air DB temp. (F)		Total Cap. [MBH]	Return Air WB Temperature [F]						
		Outdoor Temperature [F]	65.00	67.00	68.00	71.00	74.00	77.00	80.00
		75.00	54000.00	55533.33	56300.00	58333.33	60366.67	62400.00	64433.33
81.50	54038.33	85.00	51900.00	53233.33	53900.00	55933.33	57966.67	60000.00	62033.33
		95.00	49500.00	50900.00	51600.00	53633.33	55666.67	57700.00	59733.33
		105.00	47400.00	48666.67	49300.00	51366.67	53433.33	55500.00	57566.67
		115.00	45100.00	46366.67	47000.00	49066.67	51133.33	53200.00	55266.67
		125.00	42800.00	44066.67	44700.00	46766.67	48833.33	50900.00	52966.67

		Sens. Cap. [MBH]	Return Air WB Temperature [F]						
		Outdoor Temperature [F]	65.00	67.00	68.00	71.00	74.00	77.00	80.00
		75.00	37303.18	34756.16	33498.28	29575.43	26762.63	21930.40	17172.32
		85.00	36255.24	33628.31	32339.19	28694.74	25011.24	21142.11	20256.92
		95.00	35241.49	32518.00	31177.29	27451.96	23838.90	20400.38	15687.26
		105.00	33600.68	31326.64	30205.34	27074.24	24618.01	23767.20	19016.36
		115.00	32343.00	30026.20	28880.04	26128.25	23921.18	23116.56	18372.45
		125.00	32147.28	29591.59	28330.33	24817.21	21386.43	18213.50	13480.37

		Power [W]	Return Air WB Temperature [F]						
		Outdoor Temperature [F]	65.00	67.00	68.00	71.00	74.00	77.00	80.00
		75.00	6040.00	6126.67	6170.00	6296.67	6423.33	6550.00	6676.67
81.50	6226.33	85.00	6200.00	6280.00	6320.00	6450.00	6580.00	6710.00	6840.00
		95.00	6340.00	6426.67	6470.00	6600.00	6730.00	6860.00	6990.00
		105.00	6500.00	6573.33	6610.00	6743.33	6876.67	7010.00	7143.33
		115.00	6640.00	6726.67	6770.00	6900.00	7030.00	7160.00	7290.00
		125.00	6800.00	6880.00	6920.00	7050.00	7180.00	7310.00	7440.00

		SHR	Return Air WB Temperature [F]						
		Outdoor Temperature [F]	65.00	67.00	68.00	71.00	74.00	77.00	80.00
		75.00	0.69	0.63	0.59	0.51	0.44	0.35	0.27
81.50	0.63	85.00	0.70	0.63	0.60	0.51	0.43	0.35	0.33
		95.00	0.71	0.64	0.60	0.51	0.43	0.35	0.26
		105.00	0.71	0.64	0.61	0.53	0.46	0.43	0.33
		115.00	0.72	0.65	0.61	0.53	0.47	0.43	0.33
		125.00	0.75	0.67	0.63	0.53	0.44	0.36	0.25

		COP	Return Air WB Temperature [F]						
		Outdoor Temperature [F]	65.00	67.00	68.00	71.00	74.00	77.00	80.00

Total Cooling Capacity Regression Analysis

WB Temp (F)	Outdoor Temp (F)	Total Capacity	WB Temp (C)	WB Temp ^2	Outdoor Temp (C)	Outdoor Temp^2	WB Temp * Outdoor Temp	Normalized Total Cap
65.00	75.00	54000.00	18.33	336.11	23.89	570.68	437.96	1.06
65.00	85.00	51900.00	18.33	336.11	29.44	866.98	539.81	1.02
65.00	95.00	49500.00	18.33	336.11	35.00	1225.00	641.67	0.97
65.00	105.00	47400.00	18.33	336.11	40.56	1644.75	743.52	0.93
65.00	115.00	45100.00	18.33	336.11	46.11	2126.23	845.37	0.89
65.00	125.00	42800.00	18.33	336.11	51.67	2669.44	947.22	0.84
67.00	75.00	55533.33	19.44	378.09	23.89	570.68	464.51	1.09
67.00	85.00	53233.33	19.44	378.09	29.44	866.98	572.53	1.05
67.00	95.00	50900.00	19.44	378.09	35.00	1225.00	680.56	1.00
67.00	105.00	48666.67	19.44	378.09	40.56	1644.75	788.58	0.96
67.00	115.00	46366.67	19.44	378.09	46.11	2126.23	896.60	0.91
67.00	125.00	44066.67	19.44	378.09	51.67	2669.44	1004.63	0.87
68.00	75.00	56300.00	20.00	400.00	23.89	570.68	477.78	1.11
68.00	85.00	53900.00	20.00	400.00	29.44	866.98	588.89	1.06
68.00	95.00	51600.00	20.00	400.00	35.00	1225.00	700.00	1.01
68.00	105.00	49300.00	20.00	400.00	40.56	1644.75	811.11	0.97
68.00	115.00	47000.00	20.00	400.00	46.11	2126.23	922.22	0.92
68.00	125.00	44700.00	20.00	400.00	51.67	2669.44	1033.33	0.88
71.00	75.00	58333.33	21.67	469.44	23.89	570.68	517.59	1.15
71.00	85.00	55933.33	21.67	469.44	29.44	866.98	637.96	1.10
71.00	95.00	53633.33	21.67	469.44	35.00	1225.00	758.33	1.05
71.00	105.00	51366.67	21.67	469.44	40.56	1644.75	878.70	1.01
71.00	115.00	49066.67	21.67	469.44	46.11	2126.23	999.07	0.96
71.00	125.00	46766.67	21.67	469.44	51.67	2669.44	1119.44	0.92
74.00	75.00	60366.67	23.33	544.44	23.89	570.68	557.41	1.19
74.00	85.00	57966.67	23.33	544.44	29.44	866.98	687.04	1.14
74.00	95.00	55666.67	23.33	544.44	35.00	1225.00	816.67	1.09
74.00	105.00	53433.33	23.33	544.44	40.56	1644.75	946.30	1.05
74.00	115.00	51133.33	23.33	544.44	46.11	2126.23	1075.93	1.00
74.00	125.00	48833.33	23.33	544.44	51.67	2669.44	1205.56	0.96
77.00	75.00	62400.00	25.00	625.00	23.89	570.68	597.22	1.23
77.00	85.00	60000.00	25.00	625.00	29.44	866.98	736.11	1.18
77.00	95.00	57700.00	25.00	625.00	35.00	1225.00	875.00	1.13
77.00	105.00	55500.00	25.00	625.00	40.56	1644.75	1013.89	1.09
77.00	115.00	53200.00	25.00	625.00	46.11	2126.23	1152.78	1.05
77.00	125.00	50900.00	25.00	625.00	51.67	2669.44	1291.67	1.00

Figure 3.15 Regression Analysis Spread Sheet

Output

SUMMARY OUTPUT

Regression Statistics	
Multiple R	0.999640289
R Square	0.999280708
Adjusted R Square	0.999180806
Standard Error	0.007695344
Observations	42

ANOVA

	df	*SS*	*MS*	*F*	*Significance F*
Regression	5	2.961697401	0.59234	10002.6	1.68566E-55
Residual	36	0.002131859	5.9E-05		
Total	41	2.96382926			

	Coefficients	*Standard Error*	*t Stat*	*P-value*	*Lower 95%*	*Upper 95%*	*Lower 95.0%*	*Upper 95.0%*
Intercept	0.902146743	0.101487901	8.8892	1.3E-10	0.696319741	1.107973745	0.696319741	1.107973745
X Variable 1	-0.031069115	0.008477873	-3.66473	0.00079	-0.048263039	-0.013875191	-0.048263039	-0.013875191
X Variable 2	0.000683764	0.000184741	3.70121	0.00071	0.000309092	0.001058435	0.000309092	0.001058435
X Variable 3	0.010911375	0.001521955	7.16931	2E-08	0.007824706	0.013998044	0.007824706	0.013998044
X Variable 4	0.000387989	1.54232E-05	25.1562	1.9E-24	0.00035671	0.000419269	0.00035671	0.000419269
X Variable 5	-0.000605484	4.40069E-05	-13.7588	6.6E-16	-0.000694734	-0.000516234	-0.000694734	-0.000516234

Figure 3.16 Result of Regression Analysis and Corresponding Biquadratic Coefficients

Once the required data is gathered, HVAC system loop can be modeled into OpenStudio by using its GUI drag-and-drop interface. Since the air conditioning unit has single speed cooling coil, constant speed fan, and no heating component, the loop can be configured as shown in Figure 3.17. Properties from specification table and performance curve coefficients are inserted to cooling coil and fan component. At the lower side of the loop, a duct is installed to provide the conditioned air to desired thermal zone, which is connected to the living zone. This completes the ECU system setup and the resulting simulation provides HVAC power consumption as an output.

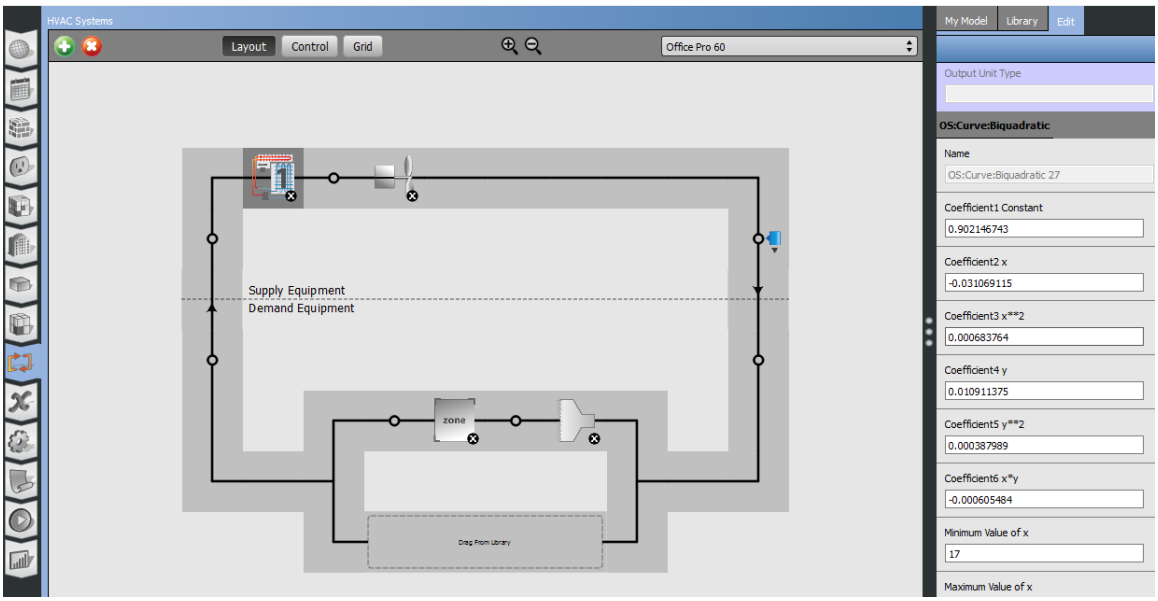

Figure 3.17 OpenStudio HVAC Tab Showing Generated Loop

3.1.6 Ground Coupling Model

As mentioned above, only having a thin layer of material adjacent to the ground, the effect of ground temperature and heat transfer through floor surface is significant in determining overall thermal energy performance of the shelter. One approach of modeling the ground coupling of the shelter is to model the floor construction by including 1 meter depth of soil, using the material properties of the soil as a material object input, and including it as an outermost layer of material of floor construction [20]. In addition, use of OtherSideCoefficient object in EnergyPlus allows the surface temperature of outer surface (which will physically represent a point of soil 1 meter underground) to be set to the actual ground temperature at 1 meter depth, where the monthly ground temperature data at different depth can be found in the EPW weather file of certain location. However, due to large mass of soil as a material as opposed to very thin layer of floor liner, it resulted in unstable simulation and it caused calculation convergence error forcing the simulation to

be aborted [20]. One way to resolve this issue is to simply remove the thin layer of shelter material, but this will lower the accuracy of the model compared to actual shelter configuration. Another approach is to use built in ground modeling object provided by EnergyPlus named GroundTemperature:Undisturbed:KusudaAchenbach. This object is based on the correlation by Kusuda and Achenbach (1965) [15], and requires input of the soil thermal conductivity, density and specific heat. The correlation then calculates the soil surface temperature using Equation (7)

$$T(z,t) = \overline{T_s} - \Delta\overline{T_s} \cdot e^{-z\cdot\sqrt{\frac{\pi}{\alpha\tau}}} \cdot \cos\left(\frac{2\pi t}{\alpha t} - \theta\right) \quad (7)$$

where *T(z, t)* is the undisturbed ground temperature as a function of time and depth, $\overline{T_s}$ is the average annual soil surface temperature in degree C, $\Delta\overline{T_s}$ is the amplitude of the soil temperature change throughout the year, θ is the phase shift, or day of minimum surface temperature α [m^2/s] is the thermal diffusivity of the ground, and τ is time constant of 365[days]. With input of GroundTemperature:Shallow object, which is an object with strings of monthly ground temperature value at 0.5m depth (can also be found in EPW file), The KusudaAchenbach module automatically calculates input of soil temperature amplitude, average soil surface temperature, and phase shift value [27, 28].

A shortcoming of this approach is that above objects cannot be inserted inside OpenStudio graphic user interface. Therefore, an EnergyPlus Measure script has to be written to specifically insert the required object. Using the measure script, OpenStudio will insert the objects following the instructions written in the scripts after the translation of the OpenStudio model into EnergyPlus IDF input file, but before the actual EnergyPlus engine

runs the simulation. This will enable the simulation to use EnergyPlus exclusive object while remaining inside the OpenStudio application for all other inputs. Figure 3.18 shows the part of the EnergyPlus measure script as an example. The script contains two major input blocks of EnergyPlus idf objects, which are shown in line 6 to line 43. Last five lines are showing a script which inserts the given objects into the OpenStudio model.

```
    # add GroundModel
    if ask_GroundModel.eql?("yes")
    baseX_string << "
!-   ===========  ALL OBJECTS IN CLASS: SITE:GROUNDTEMPERATURE:UNDISTURBED:KUSUDAACHENBACH ===========

Site:GroundTemperature:Undisturbed:KusudaAchenbach,
    KATemp 1,                !- Name
    1,                       !- Soil Thermal Conductivity {W/m-K}
    1400,                    !- Soil Density {kg/m3}
    1000,                    !- Soil Specific Heat {J/kg-K}
    ,                    !- Average Soil Surface Temperature {C}
    ,                    !- Average Amplitude of Surface Temperature {deltaC}
    ;                      !- Phase Shift of Minimum Surface Temperature {days}


      "

    baseX_string << "
!-   ===========  ALL OBJECTS IN CLASS: SITE:GROUNDDOMAIN:SLAB ===========

Site:GroundDomain:Slab,
    Shelter Ground Model,    !- Name
    5,                       !- Ground Domain Depth {m}
    1,                       !- Aspect Ratio
    5,                       !- Perimeter Offset {m}
    1,                       !- Soil Thermal Conductivity {W/m-K}
    1400,                    !- Soil Density {kg/m3}
    1000,                    !- Soil Specific Heat {J/kg-K}
    30,                      !- Soil Moisture Content Volume Fraction {percent}
    50,                      !- Soil Moisture Content Volume Fraction at Saturation {percent}
    Site:GroundTemperature:Undisturbed:KusudaAchenbach,  !- Undisturbed Ground Temperature Model Type
    KATemp 1,                !- Undisturbed Ground Temperature Model Name
    1,                       !- Evapotranspiration Ground Cover Parameter
    GroundCoupledOSCM,       !- Slab Boundary Condition Model Name
    OnGrade,                 !- Slab Location
    ,                        !- Slab Material Name
    No,                      !- Horizontal Insulation
    ,                        !- Horizontal Insulation Material Name
    ,                        !- Horizontal Insulation Extents
    ,                        !- Perimeter Insulation Width {m}
    No,                      !- Vertical Insulation
    ,                        !- Vertical Insulation Material Name
    ,                        !- Vertical Insulation Depth {m}
    Timestep;                !- Simulation Timestep
    "

    end


    # insert string to idf
    baseX_string.each do |baseX_string|

      idfObject = OpenStudio::IdfObject::load(baseX_string)
      object = idfObject.get
      wsObject = workspace.addObject(object)
```

Figure 3.18 Example of EnergyPlus Measure Script

3.2 Field Measurements

This section will present the process of measuring shelter energy usage data, performed using a military shelter physically deployed at an outdoor site. The purpose of the measurement is to gather data in the actual operating conditions, which is to be compared with OpenStudio model simulation result in order to validate the fidelity of the developed shelter model.

Off Grid Shelter LLC, as a part of Consortium for Optimally Resource-Secure Outposts (CORSO) program, led the field test. Off Grid Shelter purchased an HDT Base-X 305, and deployed the shelter in a test field located in Strafford, NH. The Base-X 305 shelter was chosen for this study since it is expeditionary shelter product widely used in deployed FOBs [30].

Figure 3.19 Deployed HDT Base-X 305 Shelter [30]

In addition, the 18’ x 25’ size is a standard military shelter produced by various vendors, thus the results represent wide variety of shelters. The Base-X 305 shelter is a lightweight and rapid deploying soft-walled shelter with folding frame, and can inhabit 12 to 14 personnel. Figure 3.19 shows the set up process of the Base-X 305 shelter in the Strafford test field, and completely deployed structure.

Measurement was done during a 17 day period, starting from August 19th 12PM, and until September 9th by the end of the day. Table 3.4 shows detailed schedule of the field measurement, and location of four metering devices used to measure temperatures at a point location. The entire period is considered as cooling period, where cooling loads are measured under hot environmental conditions.

Table 3.4 Metering Schedule of Field Deployed Shelter

Date	Configuration	Location of Meter			
		Sensor 1	Sensor 2	Sensor 3	Sensor 4
8/19	Tent Closed, Unoccupied, No AC, Temp Only, 12 pm start time	Outside	Floor Level	Ceiling Level	Above Liner
8/20	Tent Closed, Unoccupied, No AC, Temp Only	Outside	Floor Level	Ceiling Level	Above Liner
8/21	Tent Closed, Unoccupied, No AC, Temp Only	Outside	Floor Level	Ceiling Level	Above Liner
8/22	Tent Closed, Unoccupied, No AC, Temp Only	Outside	Floor Level	Ceiling Level	Above Liner
8/23	Tent Closed, Unoccupied, No AC, Temp Only	Outside	Floor Level	Ceiling Level	Above Liner
8/24	Tent Closed, Unoccupied, Yes AC, Temp and Load on AC	Outside	Supply	Return	Tent Center
8/25	Tent Closed, Unoccupied, Yes AC, Temp and Load on AC	Outside	Supply	Return	Tent Center
8/26	Tent Closed, Unoccupied, Yes AC, Temp and Load on AC	Outside	Supply	Return	Tent Center
8/27	Tent Closed, Unoccupied, Yes AC, Temp and Load on AC	Outside	Supply	Return	Tent Center
8/28	Tent Closed, Unoccupied, Yes AC, Temp and Load on AC, 12 pm start time	Outside	Supply	Return	Tent Center
8/29	Tent Closed, Unoccupied, Yes AC, Temp and Load on AC	Outside	Supply	Return	Tent Center
8/30	Tent Closed, Unoccupied, Yes AC, Temp and Load on AC	Outside	Supply	Return	Tent Center
8/31	Tent Closed, Occupied, Yes AC, Temp and Load on AC, 3:30 start time	Outside	Supply	Return	Tent Center
9/1	Tent Closed, Occupied, Yes AC, Temp and Load on AC	Outside	Supply	Return	Tent Center
9/2	Tent Open, Unoccupied, No AC, Temp Only, 8:30 am start time	Outside	Supply	Return	Tent Center
9/8	Baseline Prototype, Closed, Unoccupied, Yes AC, Temp and Load on AC	Outside	Supply	Return	Above Liner
9/9	HE Prototype, Closed, Unoccupied, Yes AC, Temp and Load on AC	Outside	Supply	Return	Above Liner

Among the measured dates, two periods are of interest. First is Aug 18th – 23th, where the temperature at different location is measured while the shelter is left unconditioned (no A/C), and the indoor temperature drifting due to outdoor weather. The other is Aug 24th –

Sept 30th, where the shelter is equipped with air conditioning unit, and temperatures are measured. During this second period, the electric load on the air conditioning system is also measured. In addition to the Base-X 305 shelter, Off Grid Shelter performed a study on a small prototype shelter for effectiveness of a newly developed insulation material. However, those results are presented in separate report and will not be covered in this study.

A temporary weather station was set up near the test site to record the weather data required by OpenStudio simulation. The measurements included dry bulb and wet bulb temperatures, humidity, wind speed, wind direction, and solar radiation. All measurements were recorded at a minute intervals. Figure 3.20 and Figure 3.21 show the measured hourly averaged indoor temperature and outdoor dry bulb temperature, respectively.

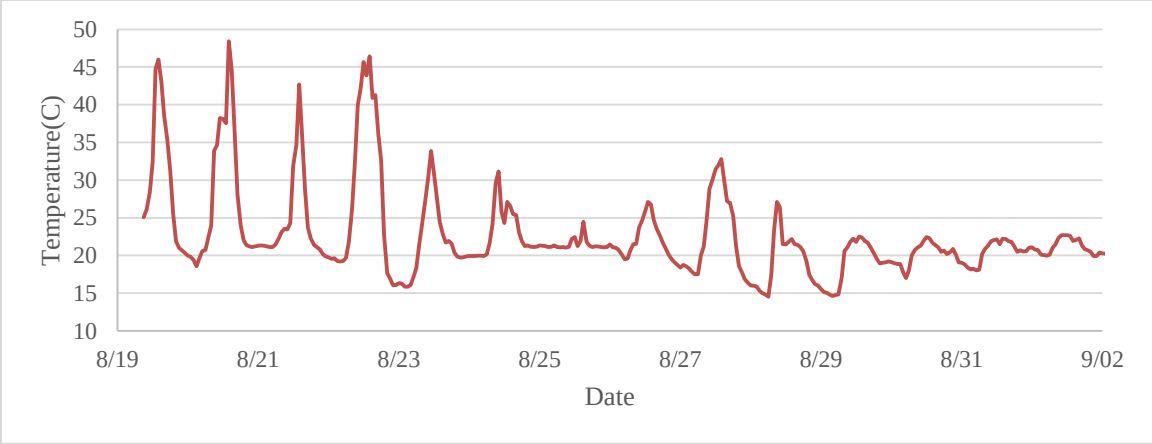

Figure 3.20 Indoor Dry Bulb Temperature During Measuring Period [30]

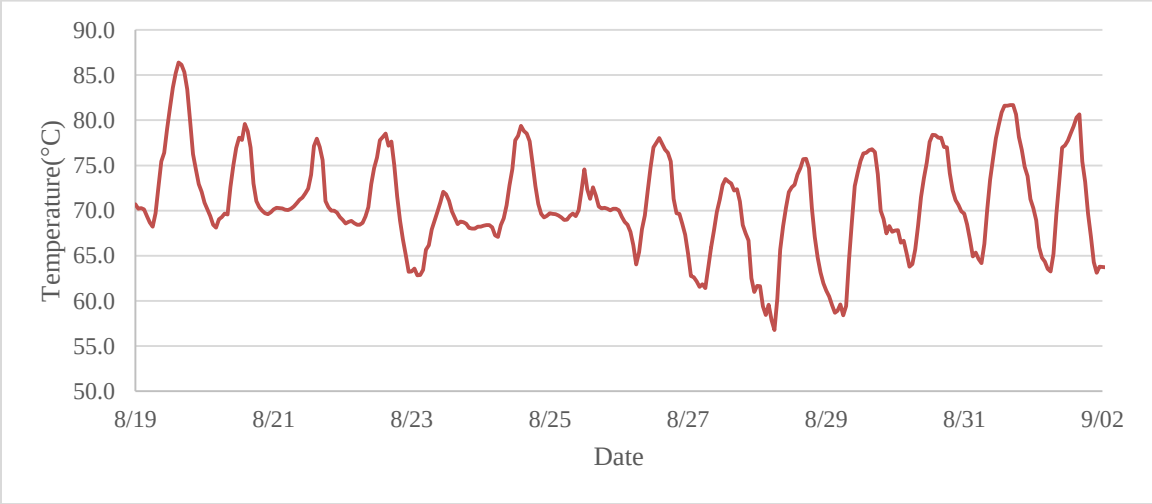

Figure 3.21 Outdoor Dry Bulb Temperature During Measuring Period [30]

3.3 Validation and Discussion

Comparing results from the OpenStudio model with various inputs generated in section 3.1 and measured data acquired by Off Grid Shelters, validation was performed with two different conditions of the measurement periods.

3.3.1 Unconditioned Period

In the earlier part of the measurement period, dry bulb temperature and humidity data were collected for five consecutive days, without any HVAC system installed (unconditioned). Since there was no control of the indoor air, the temperature and humidity were left to drift in response to outside conditions, including weather and ground temperature. By comparing the temperature of the indoor air from field measured data and OpenStudio simulations during this period, it allows validation of model predictions for given weather inputs, including ambient temperature, solar radiation, and ground temperature. It also validates whether the internal loads and infiltration are modelled correctly. The resulting temperature comparison shown in Figure 3.22 shows that the simulated result follows the trend of the measured temperature. The magnitude of the temperature peaks are also close, with maximum of about 4°C difference between highest temperatures of the day. The average error is 2.98(°C). From this result it is possible to conclude that the weather, ground temperature and load inputs are reliable so that the simulation can represent the actual shelter performance.

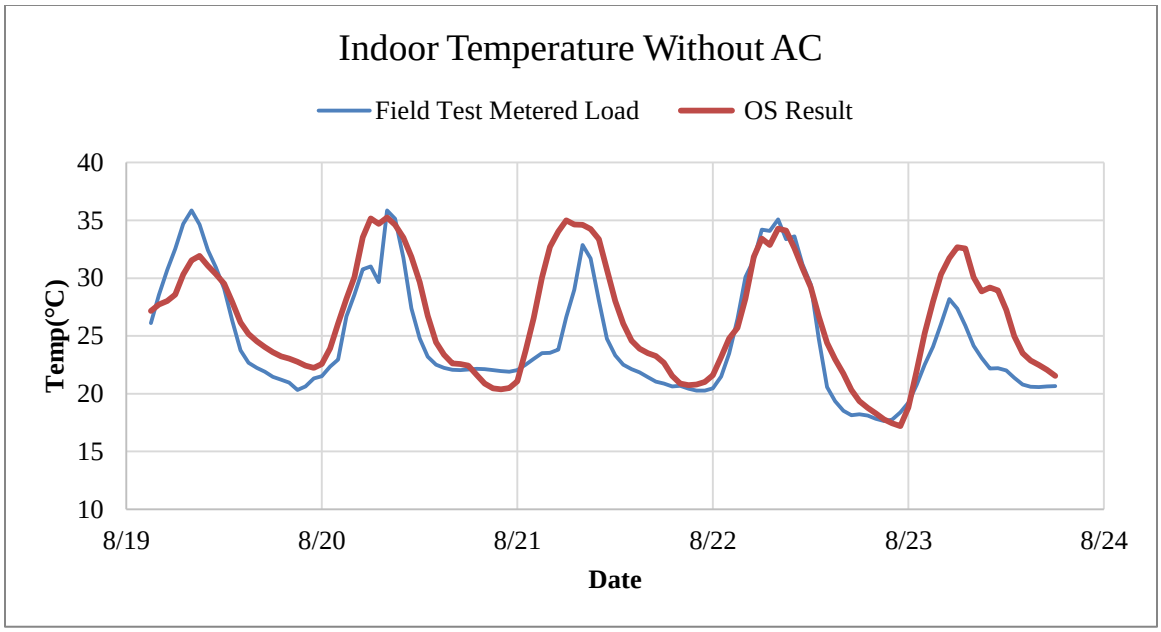

Figure 3.22 Unconditioned Indoor Air Temperature

3.3.2 Cooling Period

The second period of interest is the following six days, where the measurements were made with HVAC system installed to provide conditioned air inside the shelter living zone operating in cooling mode. This period can be called cooling period or conditioned period, since the indoor air is conditioned to meet the set point temperature. According to the report provided by Off Grid Shelters [30], the set point temperature of the cooling unit was set to 21°C (70°F) throughout the cooling period. Temperature and humidity data, as well as ECU power load were measured during this time. The main purpose of this period is to compare the HVAC system cooling load in order to verify that the input to the HVAC characteristic is accurate. Due to multiple uncertain variables such as fan operating period, difference in acceptable cooling dead-zone between actual cooling equipment and the

modelled HVAC loop, and etc., there has been a challenge in trying to compare and calibrate both indoor temperature and HVAC cooling load at the same time.

Since the main objective is to compare the cooling load, the measured indoor temperature were hard-inputs to the simulation indoor temperature, and the resulting HVAC cooling loads were compared. In order for the simulated indoor temperature to follow the measured data, hourly schedules were given to thermostat set point, which follow the measured temperature. By doing so, the HVAC system will just meet the temperature set point input, which will result in similar HVAC system behavior to the measured condition, without having excessive or insufficient cooling during the same time step. Furthermore, to sync the actual HVAC running time, ECU availability schedules were given during each day so that the cooling period matches actual run period. The result is shown in Figure 3.23.

A gap between 8/27 and 8/28 is due to HVAC load data being unavailable during that time. The result suggests that overall trend of the cooling load follows the measured data, however, there are differences in the peak load period of each day for first three days of measurement. The fact that simulation result shows lowest peak load during hottest time of the day appears unrealistic at first. However, it was found that this result is due to the limitation of the simulation input itself. While forcing the simulated indoor temperature to a measured value, this study used a method of giving the thermostat set point value to a desired temperature, instead of directly overriding the indoor temperature value. This caused the HVAC to operate only to the extent where it meets the hard-coded set point. However, this is only valid when the outside temperature is higher than the desired set point. In this case, the cooling system will constantly try to keep the temperature down to

the set point, while the higher outside temperature condition will simultaneously cause the indoor temperature to rise. If the indoor temperature is higher than the outdoor temperature, the indoor zone will be cooled itself by outdoor condition, not needing the air conditioner to be run. This can be confirmed by investigating Figure 3.24, where both the measured indoor temperature and outdoor temperature are plotted together, and it is observed that at the point where the indoor temperature exceeds outdoor temperature, the load plot is showing the inversed peak.

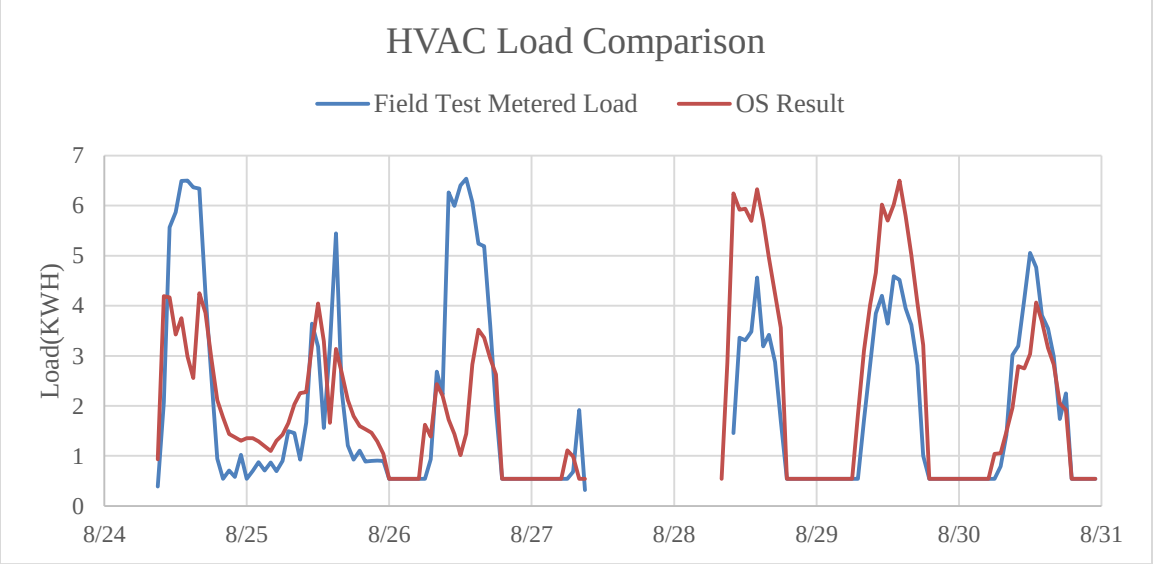

Figure 3.23 HVAC Load Comparison (Measured vs. Simulated)

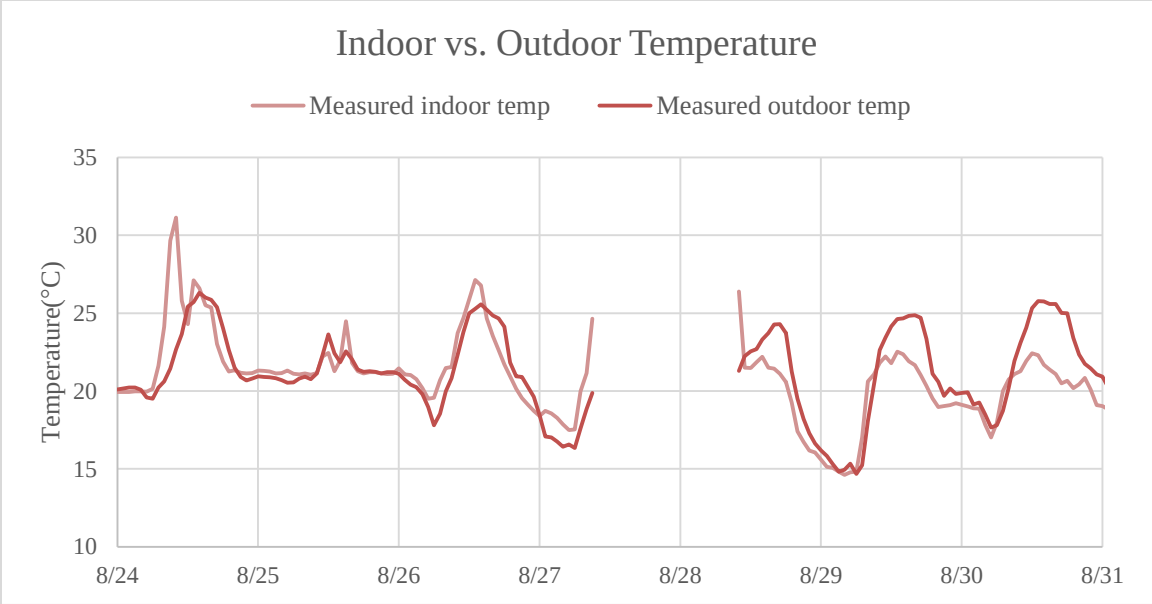

Figure 3.24 Indoor Temperature Comparison (Measured vs. Simulated)

In addition to this factor, Figure 3.25 shows that even though the indoor set point temperature was hard coded, resulting simulation output temperature does not exactly match the desired input. To resolve this issue, the indoor temperature has to be directly overridden. However, using the OpenStudio application itself there is currently no way to override the indoor temperature object, and will involve use of EnergyPlus custom code, which is beyond scope of this study.

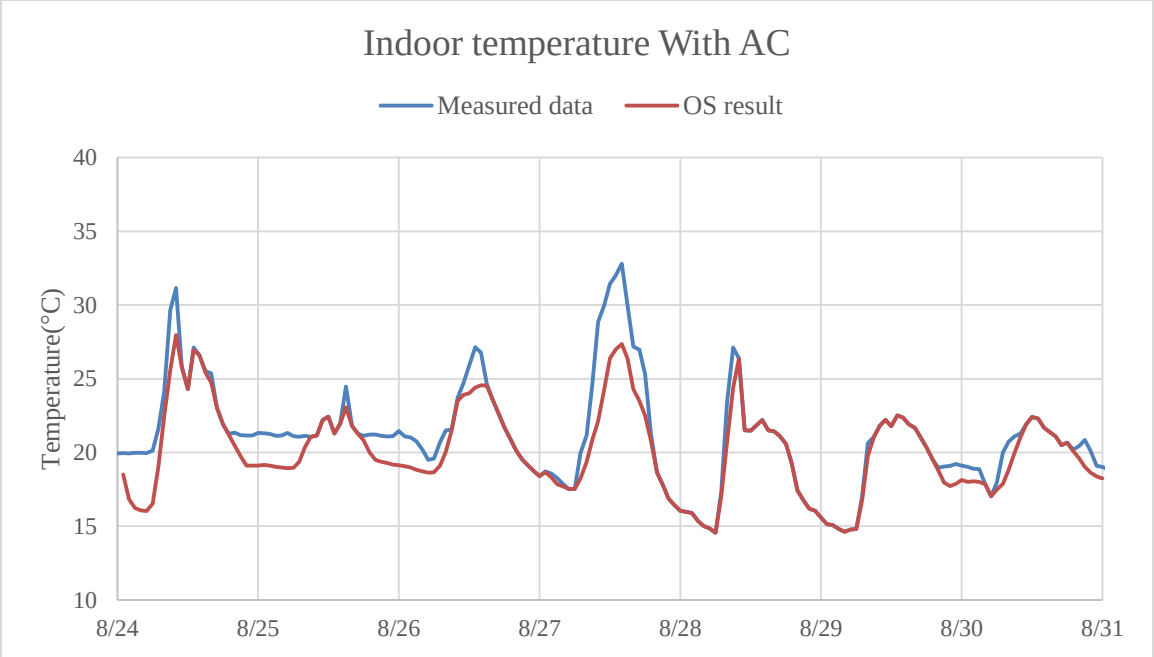

Figure 3.25 Measured and Calculated Indoor Air Temperature

To make improvements to the results without the use of custom code, the input set point was further modified. The indoor temperature set points were reverted back to the lower values only during the period where the inverted peak is observed. By doing so it was possible to acquire better agreement, as shown in Figure 3.26. Average error of this modified result is 0.64(KWH). The prediction from another OpenStudio model is provided as a reference in the figure. The Base-X305 Model that was created by NREL, and was obtained as EnergyPlus idf input. It was directly converted to an OpenStudio model and was run for the same conditions during the period.

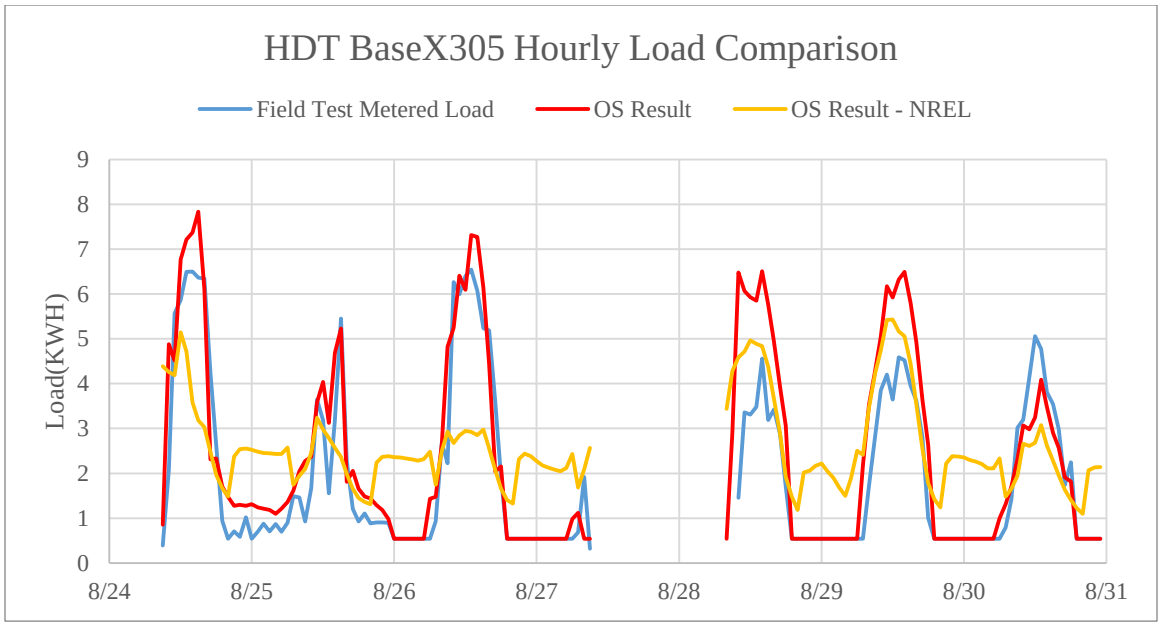

Figure 3.26 Improved HVAC Load Comparison

3.3.3 Sensitivity Analysis

In addition to the comparison with measured data, sensitivity analysis was performed with three different input variables that were assumed to have significant impact on simulation results, due to larger uncertainty. These inputs are ECU cooling capacity, infiltration values, and material R-values. Each simulation was done with varying values for each inputs, using default value, and ±50% in magnitude for the default value (30% for ECU capacity). The resulting output of the HAVC system load was compared. All simulations were done for a one week period, from 8/24 to 8/30, and without any hard inputs on schedules such as ECU operating schedule, since the purpose is only to investigate different result among simulations with alternate inputs. All other inputs such

as thermostat set point remained constant during the simulations. The results are shown in the following subsections.

3.3.3.1 ECU Cooling Capacity

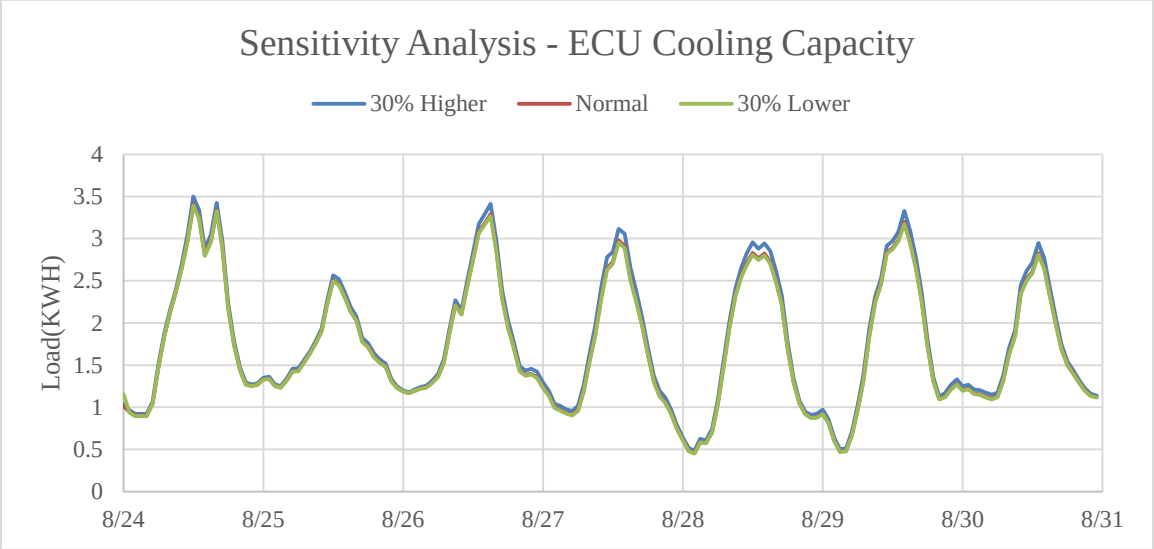

Figure 3.27 ECU Cooling Capacity Sensitivity Analysis

Figure 3.27 shows the results of sensitivity analysis using different ECU cooling capacity inputs. The output of HVAC load is largely un-affected by variations of cooling capacity inputs.

3.3.3.2 Infiltration Values

Figure 3.28 is the comparison of HVAC cooling load with different infiltration values (effective leakage area). It is shown that change in the ELA inputs shows considerable change in output values, with approximately 2.5 KWH maximum difference between highest and lowest load. The overall cooling load trend shifts upwards with higher

infiltration value, suggesting that more infiltration results in constant addition of load throughout the period. It is found that the ELA value plays a significant role in the HVAC load estimation, and therefore measuring precise value of infiltration is highly important. Conversely, it can be suggested that with other known inputs, and with field measurement data, calibration of the model can be made by adjusting the infiltration input.

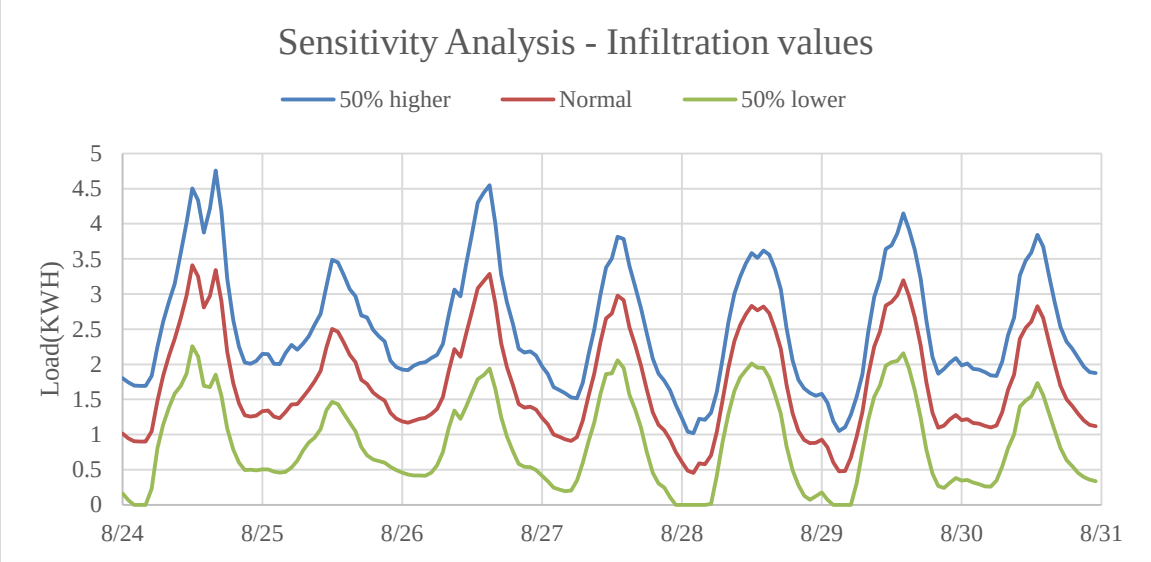

Figure 3.28 ELA Value Sensitivity Analysis

3.3.3.3 Material R-Values

The thermal resistance value of the material also had high uncertainty, since this value is significantly impacted by the interface pressure, which is typically not measured. Sensitivity analysis on different R values resulted in more cooling load required with lower R value, which means lower insulation. A notable behavior in the plots is that the difference is less significant during lower peak and intermediate periods, and becomes greater during

the peak cooling period (Figure 3.29). It can be found that insulation plays important role during hottest time of the day compared to rest of the period. In conclusion, material R value is important when estimating maximum HVAC demand, and therefore precise input is required.

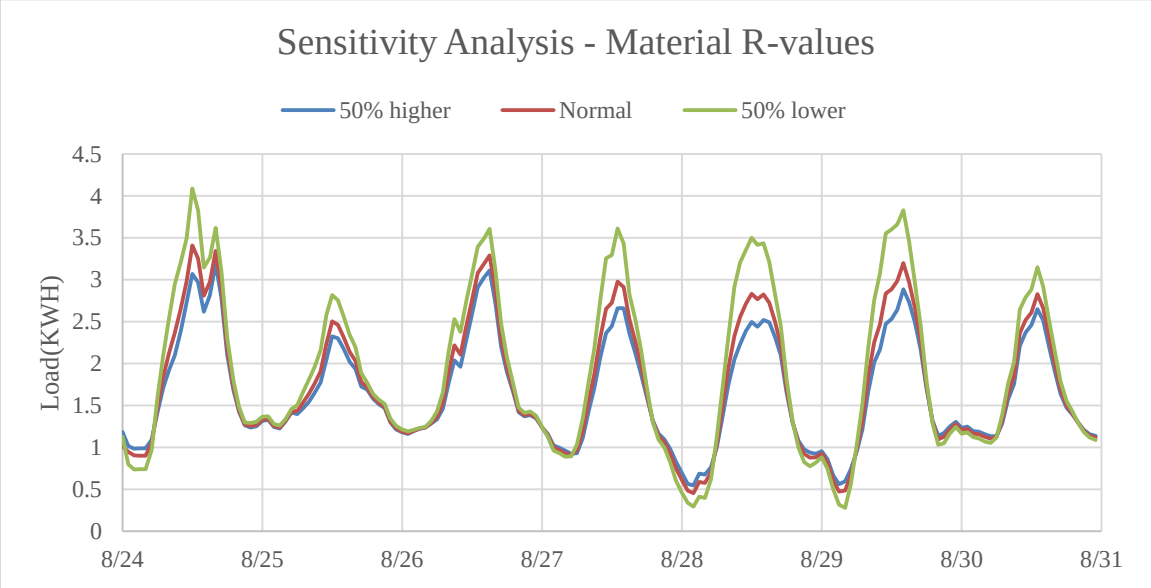

Figure 3.29 R-Value Sensitivity Analysis

3.3.4 Discussion

After generating a shelter performance model, it is important to take it through the validation, verification and calibration process. Validation is a process to compare with a reference, and to ensure that the model produces the intended result for which the model was designed, whereas verification is a procedure that focus on the correctness of the operation of a process. Calibration is based on comparison with the results to provide corrections to make the model more accurate [37, 38]. In this section, the model was

compared with the measured reference data for validation and verification purposes. The sensitivity analysis results can be used as calibration inputs to adjust the model to provide better results.

With the result of shelter modelling and validation process, it can be concluded that the proposed method of shelter modelling approach is acceptable in generating a model of military shelter using the OpenStudio. Thus, it makes it possible for military forces to estimate the operational energy demand ahead of deployment, in order to optimize the FOB configuration and fuel transportation schedule. Due to limitation of input control capability of OpenStudio explained in section 3.3.6, the resulting shelter model may have uncertainties in the HVAC load estimation output. However, this can be resolved with further investigation of custom coded inputs to the OpenStudio model, or simply by use of cooling system with sufficient cooling capability, which will result in constant indoor temperature maintained to thermostat set point without requiring indoor air temperature modification. Cause of the uncertainties will also include the measurement errors during field tests and in lab tests.

3.3.4.1 Future works

This study has focused only on the cooling period, and not on different seasons. Measurements during heating period, as well as transition period(s), with use of additional heater, or heating/cooling combined HVAC unit would be useful. Longer measurement period to acquire more data to compare with the OpenStudio simulation results would also be helpful. Furthermore, the custom code input for the OpenStudio/EnergyPlus can be investigated to give better input restriction to the model. This will include sub-hourly input

time step to enhance accuracy in the variables, such as indoor air temperature throughout the simulation period. The shelter model validation can also be done using different types of shelter and with different ECU combinations.

CHAPTER 4. APLICATION OF ADVANCED MATERIALS

In this chapter, three advanced materials in the shelter construction will be introduced. This includes an aerogel insulation, radiant barrier, and PCM material. The materials will be put in as additional layers of material at the outer surface of the interior liner (facing the gap zone), since this is a typical location where additional materials such as insulations are added in the military shelter configurations. OpenStudio simulation will be performed throughout similar period from previous chapter, and the output of HVAC electric energy load will be compared to that of baseline shelter configuration.

4.1 Aerogel Insulation

Aerogel insulation is one of the sample proprietary materials received from Off Grid Shelters (bottom right in Figure 3.5). The material is in the form of insulated coated fabric that contains aerogel. Under lab measurement described in section 3.1.2, thermal resistance value was measured to be 0.0162 m^2K/W (0.0922 ft^2*hr*F/BTU), and was introduced as new material layer in OpenStudio with no mass material. Figure 4.1 shows the results of the simulation.

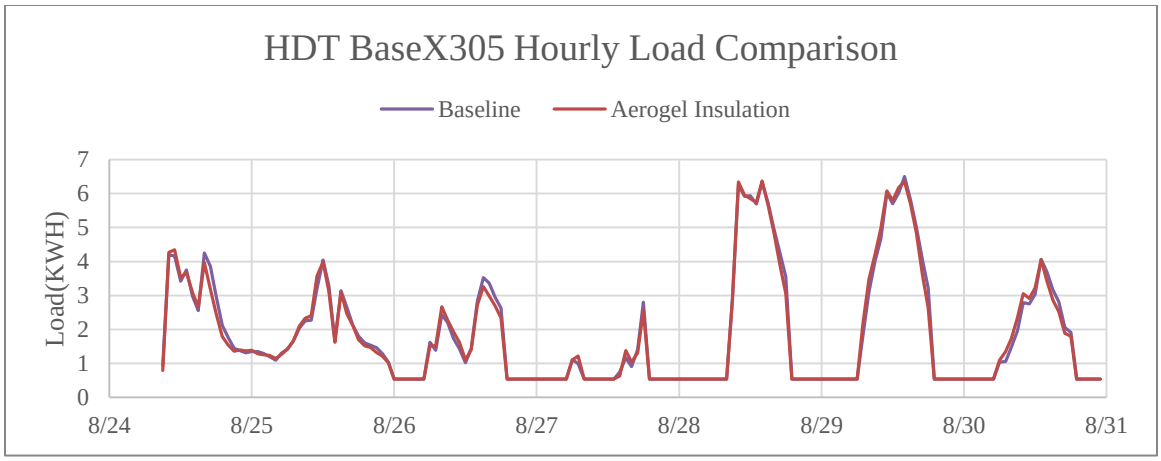

Figure 4.1 Load Comparison with Aerogel Insulation

The plot is almost identical for both conditions, with slight difference in values during peak periods. The total load over the period resulted in 298.6 KWH for baseline configuration, while aerogel insulation showed 295.7 KWH, as a result giving 0.978% of energy saving effect. It can be concluded that the aerogel insulation has no effect on reducing HVAC load, once the cost of material and installation are considered.

4.2 Radiant Barrier

Radiant Barrier is highly reflective material which can reduce thermal gain from solar radiation. The sample material received is in form of air capsules covered between reflective surfaces (top right in Figure 3.5). The no mass material object with thermal resistance value of 0.0058 m^2K/W (0.332 ft^2*hr*F/BTU) and less thermal absorptance was inserted at the outer surface of inner liner, and the OpenStudio simulation was run.

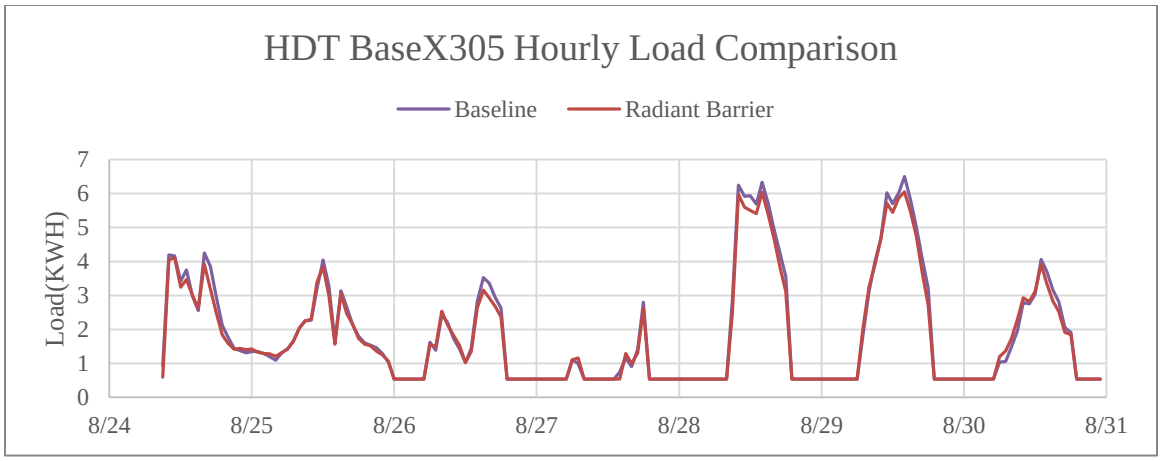

Figure 4.2 Load Comparison with Radiant Barrier

Figure 4.2 is the result of comparison between baseline HVAC load and the load from improved configuration. It can be observed that load is lower during peak periods. Overall load throughout the 7 day period was 287.96 KWH for improved configuration. Comparing with 298.62 KWH for baseline result, the use of radiant barrier gave 3.57% of energy saving. It is concluded that a modest amount of load saving was acquired with the use of radiant barrier.

4.3 PCM material

Phase change material (PCM) can act as passive thermal storage materials, by absorbing solar radiation and reducing the heat transmission to the interior. This can provide comfortable indoor air temperatures while the PCM is undergoing phase change [29]. Outlast Technologies investigated the thermal behavior of fabric integrated PCM materials for applications in military shelter systems. Measured properties of four different PCM materials were provided, based on laboratory measurements and field measurement with small model shelters. The materials are PVC laminated to woven polyester fabric, and

are coated with IR reflective/absorptive coating and latent heat storage (LHS) materials (Figure 4.3).

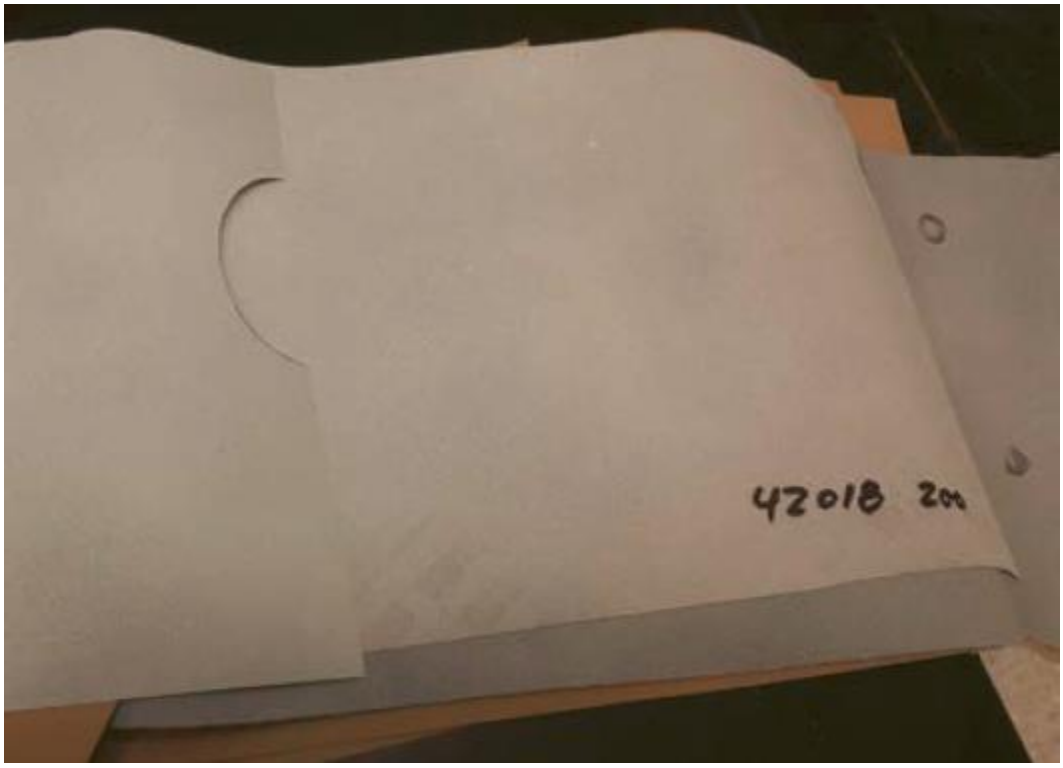

Figure 4.3 Sample Picture of Surface Coated with PCM Material [33]

Thermal properties of the material are measured, as well as thermal storage capability. The measured/calculated properties are given in Table 4.1. Control material is the PVC material without coatings.

Table 4.1 PCM Materials Properties [33]

Material Sample	Fabric wt. (g/m2)	Avg. Thick (mm)	Cp solid (J/g*K)	Cp liquid (J/g*K)	PCM Transition Temp., C	Latent Heat Prod. (J/m2)	k_avg (W/m*K)
Control	598.24	0.45	1.03	1.03	NA	NA	0.29
41005-100	679.16	0.56	1.16	1.21	35-37	14645	0.28
41005-200	792.33	0.69	1.28	1.36	35-37	31866	0.37
42018-100	689.30	0.59	1.17	1.22	42-44	15743	0.29
42018-200	826.07	0.68	1.28	1.35	42-44	34256	0.35

OpenStudio material objects are created using thermal conductivity and thickness, specific heat values. In order to give phase change and thermal storage properties of the PCM materials to the OpenStudio/EnergyPlus simulation, input of new EnergyPlus object is required. EnergyPlus supports the input of phase change material with enthalpy vs. temperature table, which can be inserted by providing few data points.

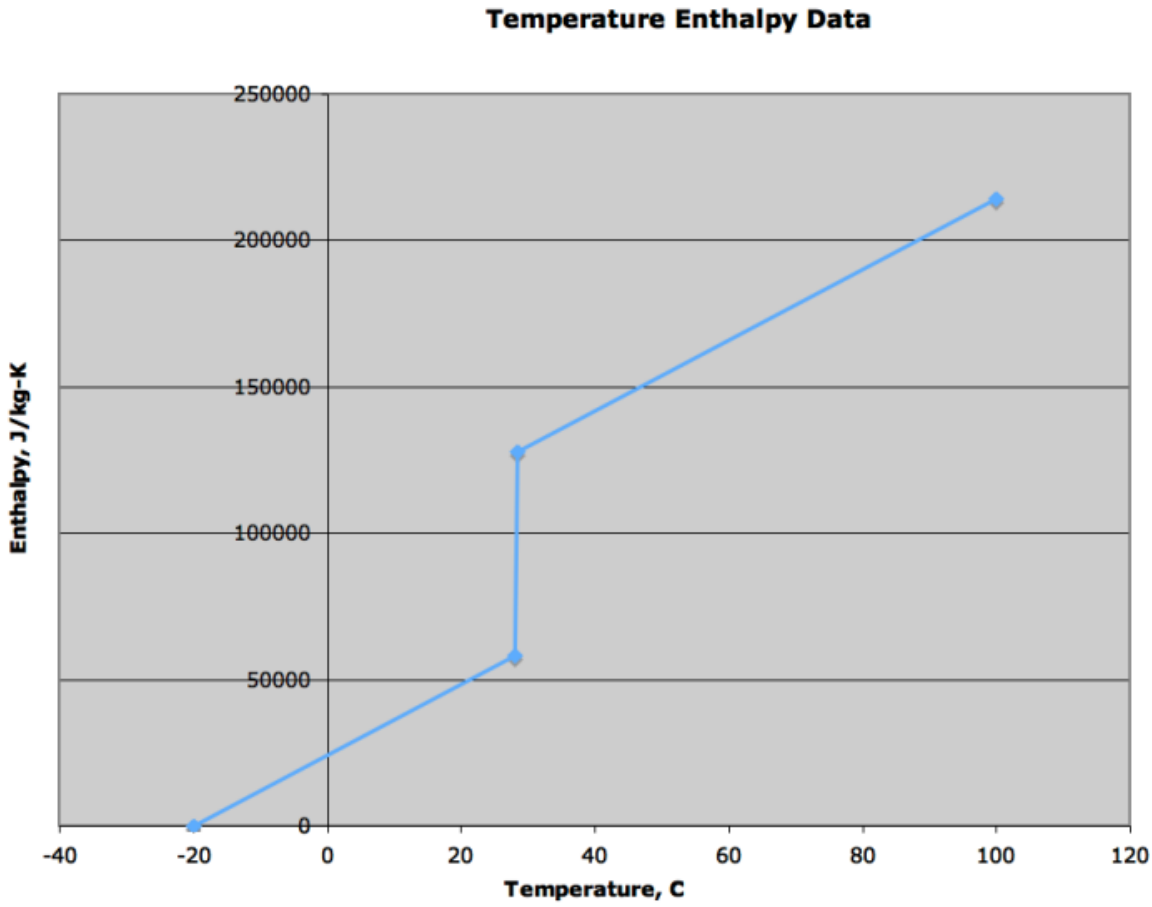

Figure 4.4 Example Plot of Temperature vs. Enthalpy [24]

EnergyPlus then generates temperature vs. enthalpy plot, and calculates the latent heat storage effect during the simulation (Figure 4.4). Four data points were generated using given Cp values, transition temperatures, and phase change latent heat. The PCM object is only supported with EnergyPlus and not with OpenStudio, therefore another EnergyPlus measure script was created to import the PCM object during the simulation. The result of one of the PCM material (41550-100) is given in Figure 4.5.

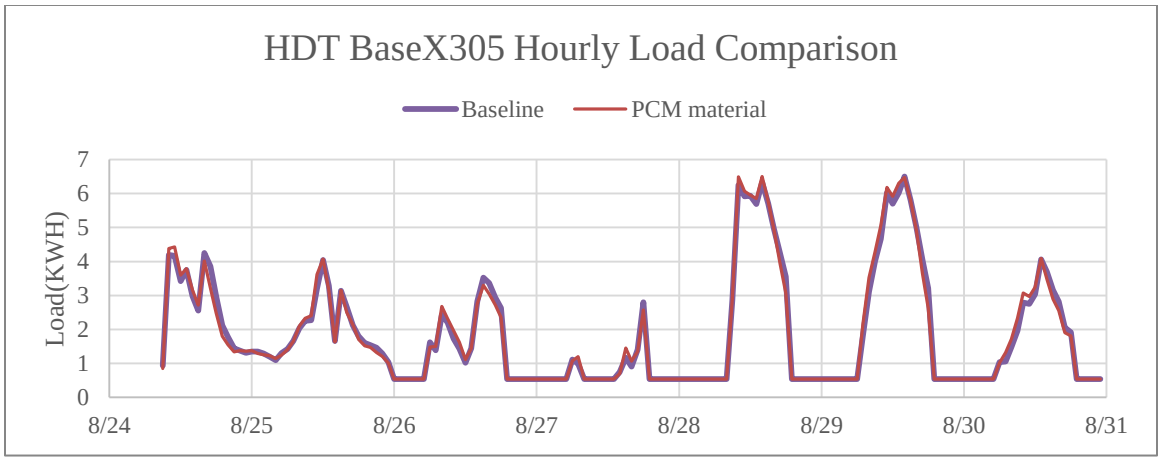

Figure 4.5 Load Comparison with PCM Material Liner

The result shows that the HVAC load performance of PCM shelter and baseline shelter gives almost identical values, with 298.62 KWH for baseline and 298.99 for PCM version. There has been 0.12% increase in the energy usage.

Even though the measurement of PCM performance showed promising latent heat storage (LHS) effect, it did not result in energy saving for the overall test period. The result may be due to the fact that the LHS effect decreases the temperature fluctuation in short time window, but does not reduce the overall heat input to the shelter in the longer period of time. In addition, previous study has found that the impact of PCM is greater in heating load compared to cooling period [20]. Further investigation of other type of PCM and the validation of input data are left as future work.

4.4 Discussion

With investigation of three different types of advanced material as additional liner to the baseline shelter envelope, it is concluded that the immediate effect of reduced HVAC energy usage was highest with the use of radiant barrier material. This is assumed to be the effect of not only the radiation reflection characteristics, but also due to smaller thermal

conductivity value among three different material types, since the radiant barrier has the largest thickness.

While using the same material, better insulation may be achieved with larger thickness. In addition, it is possible to use multiple layers of the same material, or combination of different insulation materials to enhance the overall performance of the shelter.

In addition to the result above, full year simulation was performed for each material, giving reduction in energy usage of 1.29%, 3.68%, and 0.44% for aerogel insulation, radiant barrier, and PCM respectively.

The simulation for aerogel insulation and radiant barrier was also done with different geographical locations, Atlanta, GA as a hotter location, and Denver, CO as intermediate region. In Atlanta the simulation result showed 1.21% and 4.04% decrease in energy consumption for aerogel insulation and radiant barrier respectively (Figure 4.6), and simulation in Denver resulted in 1.17% and 4.14% decrease (Figure 4.7).

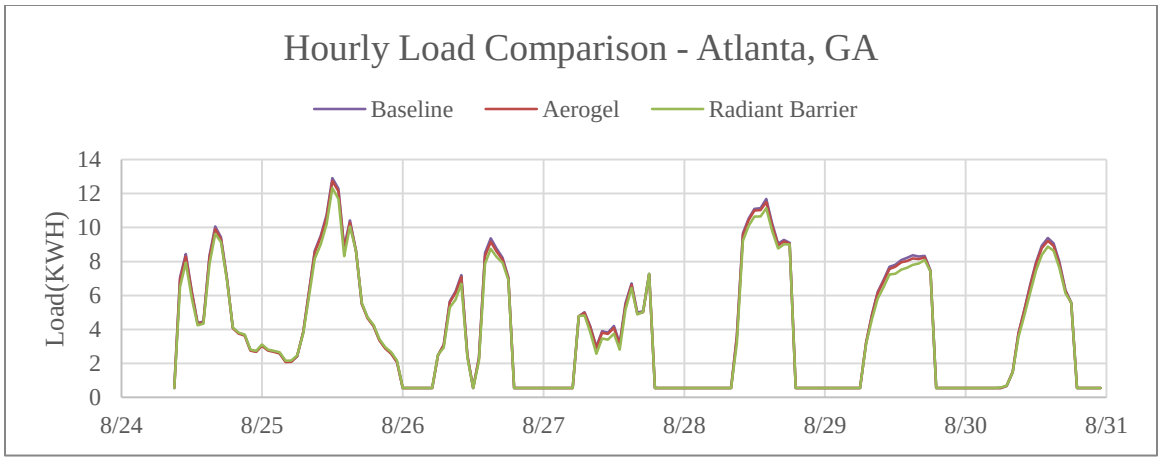

Figure 4.6 Load Comparison with Different Liners in Atlanta, GA

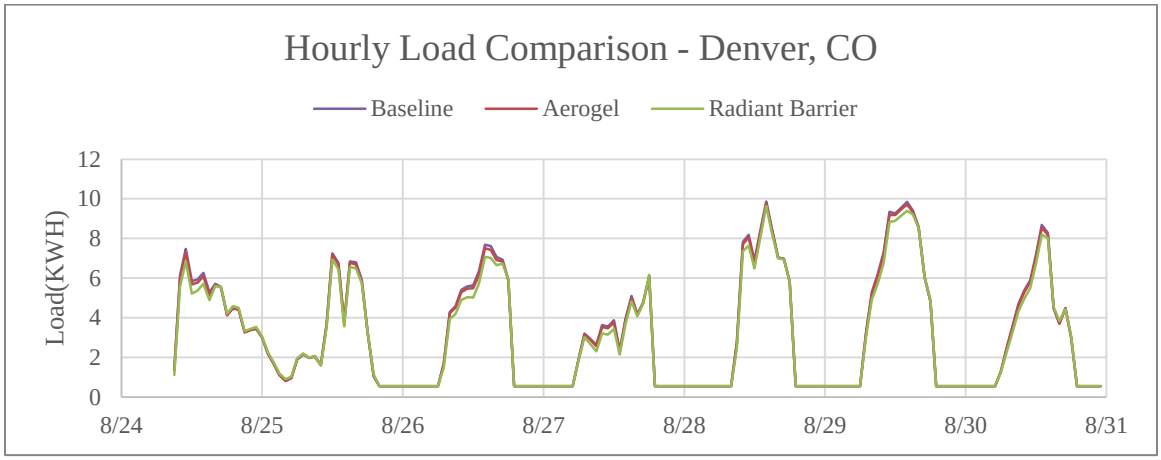

Figure 4.7 Load Comparison with Different Liners in Denver, CO

4.4.1 Future work

Since the comparison has been done for only a week in the summer season, it will be necessary to investigate the effect of each material in winter season, as well as intermediate climate. The performance should be simulated throughout the entire period,

and should be analyzed for the energy saving of each case for the whole year, and also for each season.

Further study should be performed for PCM material with given field measured values. Validation of the thermal behavior will give reliability in the PCM object input to the EnergyPlus. The study will also investigate the effect of reduction in temperature fluctuation, since this will result in better indoor comfort level and less mechanical stress to the HVAC system, even if the overall energy load does not show much difference.

REFERENCES

[1] Schwartz, M., Blakeley, K., & O'Rourke, R., "Department of Defense Energy Initiatives: Background and Issues for Congress", Library of Congress Washington DC Congressional Research Service, 2012.

[2] 112th Congress, "National Defense Authorization Act for Fiscal Year 2012," Section 2821(a), 2011.

[3] Engels, M., Boyd, P. A., Koehler, T. M., Goel, S., Sisk, D. R., Hatley, D. D., ... & Hail, J. C. (2014). "Smart and Green Energy (SAGE) for base camps final report (No. PNNL-23133)," Pacific Northwest National Laboratory (PNNL), Richland, WA (US).

[4] Alam, M., Sanjayan, J., Zou, P. X., Ramakrishnan, S., & Wilson, J. (2017). "Evaluating the passive and free cooling application methods of phase change materials in residential buildings: A comparative study," Energy and Buildings, 148, 238-256.

[5] Elarga, H., Fantucci, S., Serra, V., Zecchin, R., & Benini, E. (2017). "Experimental and numerical analyses on thermal performance of different typologies of PCMs integrated in the roof space," Energy and Buildings.

[6] Yousefi, F., Gholipour, Y., & Yan, W. (2017). "A study of the impact of occupant behaviors on energy performance of building envelopes using occupants' data," Energy and Buildings, 148, 182-198.

[7] Parker, J., Hardy, A., Glew, D., & Gorse, C. (2017). "A methodology for creating building energy model occupancy schedules using personal location metadata," Energy and Buildings.

[8] Marshall, A., Fitton, R., Swan, W., Farmer, D., Johnston, D., Benjaber, M., & Ji, Y. (2017). "Domestic building fabric performance: Closing the gap between the in situ measured and modelled performance," Energy and Buildings.

[9] Khanmirza, E., Esmaeilzadeh, A., & Markazi, A. H. D. (2017). "Design and experimental evaluation of model predictive control vs. intelligent methods for domestic heating systems," Energy and Buildings.

[10] Omar, F., Bushby, S. T., & Williams, R. D. (2017). "A Self-Learning Algorithm for Estimating Solar Heat Gain and Temperature Changes in a Single-Family Residence," Energy and Buildings.

[11] Borge-Diez, D., Colmenar-Santos, A., Mur-Pérez, F., & Castro-Gil, M. (2013), "Impact of passive techniques and clean conditioning systems on comfort and economic feasibility in low-cost shelters," Energy and Buildings, 62, 414-426.

[12] Kim, J. G., Lee, J., Ahn, B. L., Shin, H., Yoo, S., Jang, C. Y., ... & Kim, J. (2015), "Indoor Thermal Environment of Temporary Mobile Energy Shelter Houses (MeSHs) in South Korea," Energies, 8(10), 11139-11152.

[13] Cornaro, C., Sapori, D., Bucci, F., Pierro, M., & Giammanco, C. (2015), "Thermal performance analysis of an emergency shelter using dynamic building simulation," Energy and Buildings, 88, 122-134.

[14] Crawford, C., Manfield, P., & McRobie, A. (2005), "Assessing the thermal performance of an emergency shelter system," Energy and buildings, 37(5), 471-483.

[15] Ghanmi, A. (2014), "Energy management in military operational camps: A cost-benefit analysis," In Renewable Energy Congress (IREC), 2014 5th International (pp. 1-6). IEEE.

[16] Roth, A., "EnergyPlus Overcomes (Computer) Language," energy.gov/eere/buildings/articles/energyplus-overcomes-computer-language-barrier (Accessed July 9, 2017).

[17] Crawley, D. B., Lawrie, L. K., Winkelmann, F. C., Buhl, W. F., Huang, Y. J., Pedersen, C. O., ... & Glazer, J. (2001). "EnergyPlus: creating a new-generation building energy simulation program," Energy and buildings, 33(4), 319-331.

[18] Big Ladder Software, "What is EnergyPlus?" http://bigladdersoftware.com/epx/docs/8-2/getting-started/what-is-energyplus.html (Accessed July 9, 2017).

[19] OpenStudio User Documentation, "Installation and Introductory Tutorial", http://nrel.github.io/OpenStudio-user-documentation/getting_started/ (Accessed July 9, 2017).

[20] Deru, M., Bonnema, E., Barker, G., Hancock, E., & Kumar, A. (2015). "Energy Performance Measurement and Simulation Modeling of Tactical Soft-Wall Shelters (No. ERDC/CERL-TR-15-13)," Engineer Research and Development Center Champaign IL, Construction Engineering Research Lab.

[21] Keefe, D., "Blower Door Testing," The Journal of Light Construction, January 2010.

[22] Kim, M. H., Jo, J. H., & Jeong, J. W. (2013). "Feasibility of building envelope air leakage measurement using combination of air-handler and blower door," Energy and Buildings, 62, 436-441.

[23] Sherman, M. H., & Grimsrud, D. T. (1980). "Measurement of infiltration using fan pressurization and weather data," NASA STI/Recon Technical Report N, 81.

[24] EnergyPlus, "Input Output Reference: The Encyclopedic Reference to EnergyPlus Input and Output," EnergyPlus Documentation.

[25] American Society of Heating, Refrigerating and Air Conditioning Engineers. (2005). "Fundamentals," ASHRAE Handbook, p. 27.21.

[26] Judkoff, R., Polly, B., Bianchi, M., & Neymark, J. (2010). "Building energy simulation test for existing homes (BESTEST-EX); Phase 1 Test Procedure: Building Thermal Fabric Cases (No. NREL/TP--550-47427)," National Renewable Energy Lab, Golden, CO (United States).

[27] Kusuda, T., & Achenbach, P. R. (1965). "Earth temperature and thermal diffusivity at selected stations in the United States (No. NBS-8972)," National Bureau of Standards Gaithersburg MD.

[28] EnergyPlus, "Engineering Refernce: The Reference to EnergyPlus Calculations," EnergyPlus Documentation.

[29] Pasupathy, A., Velraj, R., & Seeniraj, R. V. (2008). "Phase change material-based building architecture for thermal management in residential and commercial establishments," Renewable and Sustainable Energy Reviews, 12(1), 39-64.

[30] Iacocca, M. (2015). "Baseline Energy Metering Study Summary Report (Prepared for Georgia Institute of Technology Subcontract No. RE424-S3)," Off Grid Shelters, LLC.

[31] DENSO Sales California, INC. (2008). “Service Manual Office Pro 60 (Serial Number from April 2007(0407) to Present)”

[32] HDT Global (2013). “HDT Base-X Model 305 Shelter: A Multi-Function Shelter for 12 – 14 Personnel”

[33] Hartmann, M. (2017). “Integrating Outlast LHS Materials for Exterior Structure Energy Improvements,” Outlast Technologies LLC.

[34] Omega, “ANSI and IEC Color Codes for Thermocouples, Wire and Connectors” http://www.omega.com/toc_asp/frameset.html?book=Temperature&file=tc_colorcodes (Accessed September 5, 2017).

[35] Agilent Technologies, “Dual Output Power Supply Agilent Model E3620A: Operating and Service Manual for Instruments with Serial Numbers KR71804262 and Above,” Edition 6, April 2000.

[36] Agilent Technologies, “Agilent 34970A Data Acquisition/Switch Unit,” Edition 3, March 2003.

[37] Adams, D. “Verification, Validation or Calibration” http://www.alicat.com/alicat-blog/solutions/verification-validation-calibration/ (Accessed October 19, 2017).

[38] Simpson, E. “Calibration, Validation and Verification, They Are Different You Know” https://learnaboutgmp.com/calibration-validation-and-verification-they-are-different-you-know/ (Accessed October 19, 2017).